

Dear Editor of Biogeosciences,

please find enclosed our Author's Response for manuscript entitled "A simple optical index shows spatial and temporal heterogeneity in plankton community composition during the 2008 North Atlantic Bloom" (original submission was done as "Optical community index to assess spatial patchiness during the 2008 North Atlantic Bloom") by I. Cetinić, M. J. Perry, E. D'Asaro, N. Briggs, N. Poulton, M. E. Sieracki and C. M. Lee.

In this document you will find, in following order:

- 1) Response to the reviewer #1
- 2) Response to the reviewer #2
- 3) Marked-up manuscript version

We thank you for your time,

Ivona Cetinić,

icetinic@gmail.com

Research Associate  
Ira C. Darling Marine Center  
University of Maine  
193 Clark's Cove Road  
Walpole ME 04573-3307  
USA  
Phone: +1-207-5638325  
<http://ivona-cetinic.flavors.me/>

## **Response to the reviewer #1**

We would like to thank to the reviewer for time devoted to this manuscript, comments and suggestion. Below we answer the reviewer's comments with references to appropriate parts of the text (in quotation marks). We would also like to point out to the reviewer that last name of the first author is **Cetinić**, not **Cetenic**.

*Review of Optical community index to assess spatial patchiness during the 2008 North Atlantic Bloom.*

*The author propose (and use on Glider collected data) a new optical index of phytoplankton community structure. The index appears robust at the time of year and study area that they have examined allowing them to study the spatial variability in diatom-dominated communities vs other communities in their study region.*

### **Main comments**

*While the study is interesting I am a bit uneasy when the authors attempt to interpret the index. In this aspect, I think the authors could go a little further with all the data available to them. The authors suggest that it is the higher chlorophyll to carbon ratio of diatoms that leads to variability in this index. This assumes that  $b_{bp}$  is a good estimator of phytoplankton carbon across communities. Theory suggests that it isn't (see Stramski et al. 2004 cited in the text) and that  $c_p$  is a better estimator of phytoplankton carbon (this is why it has been used multiple time to estimate phytoplankton growth rates). If their hypothesis was true we would expect a CHL  $F/c_p$  ratio to be even better. They did not present this data to support their analysis.*

Answer: Stramski et al. (2004), cited in the text, suggest – based on Mie theory– that most of the backscattering in the ocean is associated with submicron particles. However, several recently published papers question the application of theory to real world oceanic particles which are rarely perfectly spherical and of uniform internal structure. Dall'Olmo et al. (2009), using actual data not models, found that up to 50% of the  $b_{bp}$  signal in mesopelagic waters (comparable to the waters in the region reported in our manuscript) is associated with the fraction larger than 3  $\mu\text{m}$ . In my own recent experiments in the mid-latitude North Atlantic and southern Labrador Sea (Cetinić, Slade and Poulton, unpublished) we found up to 80% of  $b_{bp}$  signal was associated with the fraction of particles larger than 5  $\mu\text{m}$ . One of the main reasons that  $c_p$  (particulate attenuation coefficient) has been used multiple times to estimate phytoplankton growth rates is that  $b_{bp}$  has not been routinely measured while  $c_p$  is routinely measured. However, the measurement of backscattering is a rapidly changing field, with an almost exponentially increasing frequency of publications reporting backscattering measurements over the last few years.

With regard to carbon, several recently published papers have demonstrated that  $b_{bp}$  is a good estimator of phytoplankton carbon (Martinez-Vicente et al., 2013; Martinez-Vicente

et al., 2012) and a paper by in review by Graff (Graff, personal communication) shows a similar, strong and statistically significant *in situ* relationship between  $b_{bp}$  and phytoplankton carbon. Numerous papers by Behrenfeld and colleagues are based on the relationship between backscattering and carbon. Cetinić et al. (2012) and references provided therein show that both  $b_{bp}$  and  $c_p$  has been successfully used as a proxy for carbon.

While we agree with the reviewer that the ratio of chlorophyll fluorescence and  $c_p$  is a good proxy for community composition (as we found for the Lagrangian float and ship data), the goal of this paper is to build a reliable optical community proxy that can be used with simple optical datasets that can be collected by the gliders. With the exception of a few glider demonstration experiments with short path-length transmissometers, gliders for weight and size limitations typically do not carry instruments to measure  $c_p$ . We appreciate the confirmation by the reviewer that the index allows us “. . . to study the spatial variability in diatom-dominated communities vs other communities . . .”

*The author rejects physiology (fluorescence non-photochemical quenching and nutrient limitation, apart from Si) as a potential source of variability in the data but suggest the higher concentration of Chl per volume in larger cells would be responsible for variability in the index. This part (last paragraph of p. 12849) is very confusing to me, as the authors appear to make several leaps that are not easy to follow. The following sentence is particularly ambiguous I find: Chl per cell volume scales inversely with cell size... resulting in higher Chl-to-carbon ratios for larger cells. The changes seem to go the opposite way to me (i.e. lower Chl/C ratio in larger cells). Their strongest support for that argument originates from Fig. 5c where the ratio of Chl to autotrophic carbon is higher in communities with higher diatoms. However, it is not clear on this figure where the “Chl” comes from (fluorescence or HPL). On panel A they refer to HPLC specifically, but not on panel C which suggest that it chlorophyll from fluorescence (as in Fig 3A or 2B?).*

Answer: We reject fluorescence non-photochemical quenching as a source of variability, as all data from depths shallower than 10 meters are rejected. Figure 2C shows the relationship between fluorescence and light; quenched data are excluded. Nutrient limitation, apart from Si limitation, is not a potential source of variability; nitrate is in great excess ( $> 8 \mu\text{M}$ ) at this time of year. Although phosphate was not measured, no report from the subpolar North Atlantic has ever implicated this nutrient as a limiting nutrient. Hence we reject physiology as the explanation for the difference in the  $Chl F/b_{bp}$  ratio.

Figure 5 C uses fluorometrically-derived chlorophyll, identified as *Chl*. We thank the reviewer for pointing out that, although we thought all acronyms were clearly defined in

the Material and Methods, because of the complexity of the paper, the abbreviations are not sufficiently clear. We added a table, listing measured parameters, associated symbols and methods/instruments.

Field data supports the taxa-specific chlorophyll to carbon ratio (Fig. 5A,B); several previously published papers (Fujiki and Taguchi, 2002, and others cited in text; please see section 4.1) have demonstrated same trend that we are demonstrating here. We would appreciate learning about the references to which the reviewer refers that show “*The changes seem to go the opposite way to me (i.e. lower Chl/C ratio in larger cells)*”.

*It seems to me that the authors should look at the ratio of Chl F/ChlHPLC as a function of their % diatoms index to examine if it varies with their index. Also, authors do not discuss the lower fluorescence efficiency expected from larger cells due to pigment packaging (both for absorption and reemission).*

Answer: We report the relationship between chlorophyll fluorescence and extracted chlorophyll (Knap et al., 1996) in Fig. 2A. Color coding in this figure is the optical index for data point, clearly demonstrating that relationship between those changes when optical index reaches the highest values. High values of the optical index associate with high percentages of diatoms.

We agree with the reviewer that a reduction in the chlorophyll specific absorption coefficient and in fluorescence efficiency (fluorescence emission normalized to extracted chlorophyll concentration) is a well-documented phenomenon associated with pigment packaging (cf. Cleveland and Perry, 1987). However, we did not see a statistically significant difference in the chlorophyll specific absorption coefficient ( $a^*$ , normalized to 676 nm *sensu* Mitchell and Kiefer, 1988; data not reported here); this may have been due to the elongated shape of many of the diatoms. The important point is that even if there were a reduction in fluorescence efficiency, the difference between the diatom-dominated communities and the post diatom communities is a factor of two.

*One aspect that I found quite exciting with this paper is that it presents an in situ study showing a clear optical community index (at least for that region and time of year). This, however, brought a particularly puzzling aspect: the index varies exactly in the opposite to the way the phytoplankton functional group algorithm developed by Alvain et al. (2006). For example Brown et al. (2008) (see also [oddly] similar study by Alvain et al, 2012) showed that the Alvain et al. algorithm identifies regions with high backscattering (to chlorophyll) as composed of diatoms. I think this is worth mentioning in the paper.*

Answer: Brown et al. (2008) show that distribution of  $b_{bp}$  anomalies is similar to the ones depicting distribution of phytoplankton groups in Alvain's papers (based on PHYSAT model). However, Brown and coauthors are pointing out that the diatoms are found in the area that have high  $b_{bp}$  when compared to the global mean  $b_{bp}$ ; they are not referring to chlorophyll, as reviewer suggests. The rigorous study of backscattering is only truly beginning, and we expect new papers will report more new and intriguing results in the near future.

**Minor points.**

*p. 12838 line 18, change "volts" to "voltage"*

Answer: Volt is a derived SI unit (<http://physics.nist.gov/cuu/Units/units.html>) of electric potential difference or electromotive force; voltage is a common expression.

*Throughout - change Michaelis-Menton to Michaelis-Menten. Also check for consistency of hyphenation.*

Answer: Changes have been made throughout the text. Thank you.

*Figure 2, panel C - There appears to be photochemical quenching (PQ) of fluorescence below  $\sim 70 \mu\text{mol m}^{-2} \text{s}^{-1}$ . (i.e. a decrease in fluorescence at as light decreases). The red points (high community index), however, do not seem to be affected by this quenching. Suggesting less response to PQ in these points (i.e. physiological aspect to the index?).*

Answer: There is a slight trend and at  $0 \mu\text{mol photons m}^{-2} \text{s}^{-1}$  there is great variability. Both of these are likely due to the low biomass and therefore low signal (and high signal to noise) at these low light intensities and greater depths.

*Figure3, caption - In panel C I think you should change "line solid line" for "solid line" and "Heavy solid line" for "dashed red line".*

Answer: Changed.

*Figure 6 - I think the reader needs a bit more help interpreting this figure (this reader does anyway). I am particularly confused with what seems like to different series of points in panel A (a similar thing happens in panel B). With high community index points following the glider data and low community index points not following the glider data but taken on the same day. Were they taken in different areas? If so perhaps a different symbol would be appropriate?*

Answer: There is no glider data on this figure. As the caption states, these figures are a combination of float and ship data. Colored points were data collected by the ship's CTD

on different stations. Some of the ship CTD profiles were taken in the water of the same community composition as the float, and some of them were taken in the waters that had different community composition. This figure demonstrates large spatial heterogeneity in phytoplankton community composition on the mesoscale (ship's daily reach). We believe that caption is explanatory, and no change is needed.

*Conclusion - Although that point is alluded to, I think it should be highlighted more strongly that this index has only been validated for a very limited set of conditions. It should certainly not be used blindly elsewhere. Furthermore, the absolute values of this index are only relevant for the fluorometers used on that cruise and in the way they were intercalibrated; relationships between voltages and phytoplankton absorption will vary widely between fluorometers.*

Answer: We completely agree. In order to highlight this point, we changed the text in the conclusion to following:

“The interpretation of these ratios must be based on *in situ* validation and used within a limited set of conditions, at least until a better mechanistic understanding is developed.”

#### References:

- Alkire, M.B. et al., 2012. Estimates of net community production and export using high-resolution, Lagrangian measurements of O<sub>2</sub>, NO<sub>3</sub><sup>-</sup>, and POC through the evolution of a spring diatom bloom in the North Atlantic. Deep-Sea Research Part I-Oceanographic Research Papers, 64: 157-174.
- Alkire, M.B. et al., 2014. Net community production and export from seaglider measurements in the North Atlantic after the spring bloom. Journal of Geophysical Research: Oceans: n/a-n/a.
- Brown, C.A., Huot, Y., Werdell, P.J., Gentili, B., Claustre, H., 2008. The origin and global distribution of second order variability in satellite ocean color and its potential applications to algorithm development. Remote Sensing of Environment, 112(12): 4186-4203.
- Cetinić, I. et al., 2012. Particulate organic carbon and inherent optical properties during 2008 North Atlantic Bloom Experiment. J. Geophys. Res., 117(C6): C06028.
- Cleveland, J., and Perry, M., 1987. Quantum yield, relative specific absorption and fluorescence in nitrogen-limited *Chaetoceros gracilis*, Marine Biology, 94, 489-497.

- Dall'Olmo, G., Westberry, T.K., Behrenfeld, M.J., Boss, E., Slade, W.H., 2009. Significant contribution of large particles to optical backscattering in the open ocean. *Biogeosciences*, 6(6): 947-967.
- Fujiki, T., and Taguchi, S., 2002. Variability in chlorophyll a specific absorption coefficient in marine phytoplankton as a function of cell size and irradiance, *J. Plankton Res.*, 24, 859-874, 10.1093/plankt/24.9.859.
- Knap, A., Michaels, A., Close, A., Ducklow, H. and Dickson, A. (eds) (1996) Protocols for the Joint Global Ocean Flux Study (JGOFS) Core Measurements. JGOFS Report N. 19, vi + 170 pp. Reprint of the 10C Manuals and Guides No 29, UNESCO 1994.
- Martinez-Vicente, V., Dall'Olmo, G., Tarran, G., Boss, E., Sathyendranath, S., 2013. Optical backscattering is correlated with phytoplankton carbon across the Atlantic Ocean. *Geophysical Research Letters*, 40(6): 1154-1158.
- Martinez-Vicente, V., Tilstone, G.H., Sathyendranath, S., Miller, P.I., Groom, S.B., 2012. Contributions of phytoplankton and bacteria to the optical backscattering coefficient over the Mid-Atlantic Ridge. *Marine Ecology-Progress Series*, 445: 37-51.
- Mitchell, B. G., and Kiefer, D. A. 1988. Chlorophyll a specific absorption and fluorescence excitation spectra for light-limited phytoplankton, *Deep-Sea Research, Part 1*, 35, 639-663.
- Stramski, D., Boss, E., Bogucki, D., Voss, K.J., 2004. The role of seawater constituents in light backscattering in the ocean. *Progress in Oceanography*, 61(1): 27-56.

## Response to the reviewer #2

We thank the reviewer for the time devoted to this manuscript, and for the comments and suggestions. Below we answer the reviewer's comments with references to appropriate parts of the text (in quotation marks).

*The authors propose that the ratio between chlorophyll fluorescence (Chl F) and the particulate backscattering coefficient (bbp) is a proxy of relative contribution of diatom in plankton biomass and it can distinguish diatom community from pico- and nanophytoplankton community. This proposal is based on in situ measurements of a series of variables related to phytoplankton, taken by glider, float and ship. The authors discuss mechanisms of the co-variability between ChlF/bbp and diatom, to conclude that variability in ChlF/bbp is caused by the taxa-specific chlorophyll-to-carbon ratio of phytoplankton and that the observed highest values of ChlF/bbp are indicative of Si-limitation to diatom.*

### Main comments

*The manuscript summarizes extensive measurements of phytoplankton and associated variables relatively well. Especially, the authors' findings that the optical index can be a useful proxy of relative carbon biomass of diatom has a great potential to advance understanding of phytoplankton ecology of their study region because the optical index can be determined from in situ measurements taken by commercially-available instruments and therefore a load of measurements would easily be taken. As a result, the paper has a good potential to be published in Biogeosciences. The authors discuss mechanisms controlling variability in ChlF/bbp, to conclude that the variability is due to (1) taxa specific differences in the cellular Chl-to-autotrophic carbon ratios (2) a fraction of the planktonic carbon due to diatom (Section 4.1, L 6, P12849) and (3) Si-limitation to diatom is responsible for the highest values of ChlF/bbp (Section 4.2, L8, P12852).*

*Firstly, I am surprised that (1) and (3) (as well as (2)) are rather explicitly concluded in the main text, but not mentioned in both Abstract and Conclusion. These conclusions should be mentioned there.*

Answer: Changes have been made in Title, Abstract and Conclusion to point out to these results more clearly.

In the Abstract, we added the following sentence:

“Observed changes in optical index were driven by taxa-specific chlorophyll-to-autotrophic carbon ratios and by physiological changes in Chl F driven by the silica limitation.”

In the Conclusions we have added and modified text to the following:



The observed shift in the optical index was primarily driven by the change in phytoplankton composition and distribution of biomass, reflecting differences in taxa-specific chlorophyll-to-autotrophic carbon ratios. Furthermore, the optical index allowed us to observe changes in the physiological status of the community as well, clearly isolating the senescent, Si-limited, termination stage of the diatom bloom from surrounding patches of diatoms not yet in senescence.

*Secondly, although the conclusion (1) is exciting, it was drawn from their observation that Chl-to-autotrophic carbon ratio is higher by factor of two for diatom-dominated samples (L4, P12850). I am not really convinced as to how the authors were able to conclude the above (1) just because of that. No detailed discussion was given as to how difference in Chl-to-carbon ratio among different plankton community can be translated to variability in ChlF/bbp (only discussion on high Chl-to-carbon ratio for diatom was given). Please explain/clarify this, since it is crucial for readers to understand how the optical index proposed by the authors works.*

Answer: Section 4.1 asks the question “Why does the  $Chl F/b_{bp}$  ratio vary?” and systematically eliminates potential competing explanations for the variability in the ratio:

- 1) We reject fluorescence non-photochemical quenching as a source of the variability, as all data from depths shallower than 10 meters are rejected. Figure 2C shows the relationship between fluorescence and light; quenched data are excluded. Nutrient limitation, apart from Si limitation, is not a potential source of variability; nitrate is in great excess ( $> 8 \mu\text{M}$ ) at this time of year. Although phosphate was not measured, no report from the subpolar North Atlantic has ever implicated this nutrient as a limiting nutrient. Hence we reject physiology as the explanation for the difference in the  $Chl F/b_{bp}$  ratio.

- 2) Other field studies show higher  $Chl$ -to-carbon ratios for diatom dominated communities in contrast to communities dominated by small phytoplankton (Llewellyn et al., 2005; Putland and Iverson, 2007; Li et al., 2010).

- 3) While it could be possible that the ratio changed because heterotrophic protists became more abundant, Fig. 5D shows that changes in the percentage of heterotrophic carbon to total carbon is not driving the optical index.

We conclude – if chlorophyll fluorescence is a proxy for chlorophyll concentration (please see Fig. 2) and that if optical backscatter is a proxy for particulate organic carbon (Cetinić et al, 2012) – that higher diatom chlorophyll-to-carbon ratios are responsible for the observed higher  $Chl F/b_{bp}$  ratios.

*Thirdly, the significant scientific finding in this manuscript is, as concluded by the authors, that  $ChlF/bbp$  is an optical index of a relative abundance of diatom community. Meanwhile, the authors also introduce rather immature analysis on patchiness of the optical index, but failing to*

*draw a significant scientific finding, as the authors themselves admit it by stating “analysis on patchiness did not manage to resolve the primary drivers of the observed patchiness in community composition in the Conclusion section (see L19,P12854)”. As a result, description of patchiness does not add a value on this paper, and the section describing “patchiness” distracts the overall story of this paper. The main story and points of this paper (i.e. the optical index is a proxy of %diatom) would be much clearer without the discussions of the patchiness.*

Answer: We have, following the suggestion of the reviewer, modified the Abstract and Conclusions to put stronger emphasis on the optical index. However, we do not agree with the reviewer that our analysis of patchiness is not important and distracting. This is, to our knowledge, the first analysis of this kind, where the distribution of the phytoplankton community was assessed for a two-month period with such high spatial and temporal resolution. Without the patchiness study, this is just a methods paper. In the manuscript, we have alluded that spatial patchiness is associated with physical processes that were happening on the larger scale, and pointed to models that have demonstrated that such patchiness, in these types of systems, originates from mostly physical drivers. Our analysis did not manage to resolve the primary drivers of the patchiness primarily due to the sampling schema; hence, we could not resolve temporal from spatial variability. Secondly, due to the lack of instruments for measuring higher trophic levels (zooplankton) on the same scales, we cannot say anything about potential top-down control of this spatial patchiness. Here, we are presenting a methodology that could, in the future, in combination with different sampling schemes and a new generation of imaging/acoustic instruments, offer a better view into the forcing functions that lead to heterogeneity of oceanic biodiversity and associated biogeochemistry.

### **Other comments**

*Title The optical index is developed here, actually to estimate a relative carbon biomass of diatom. The title needs to be revised to be more precise.*

Answer: This optical index does not estimate a relative carbon biomass of diatom; rather it tells us something about plankton community type and how it changes over space and time. The variability in that ratio is driven by the taxa-specific chlorophyll-to-carbon ratio. We have changed the title to following:

**“A simple optical index shows spatial and temporal heterogeneity in plankton community composition during the 2008 North Atlantic Bloom”**

*Introduction Please re-consider the phrase “in situ remote optical sensing...as well as from space”, since Reader can easily confuse it with “optical remote sensing”. (Is “autonomous optical sensing” better in the present context?)*

Answer: Changed to read: “Autonomous observations of phytoplankton are becoming increasingly ubiquitous, including *in situ* optical sensing from Argo-type and Lagrangian floats, gliders, and moorings, as well remote sensing as from space.”

*Section 3 There are quite many variables and observation platforms appear in this section. Also different instruments, platforms, and/or data processing were applied even for a same variable (e.g. Chl, diatom carbon etc.). All measurement items, instruments, platforms and data processing methods could be better summarized, for example, in a table.*

Answer: We appreciate the reviewer’s suggestion, and now include a table with measured parameters, associated acronyms/symbols and instrument/methods for specific platforms (Table 1).

*Subsection 3.2 Please plot Si concentration, in one of the plots in Fig. 3, since it would be useful information for Reader to understand a latter discussion about Si-limitation in Section 4.2 (as well as it is an evidence for your statement L20 in P12844).*

Answer: Silicic acid is plotted in Fig. 6B on the same plot as shown in Fig. 3. We have now added: Also see Fig. 6.

### *Subsection 3.3*

*Scatter plots (otherwise a table showing correlation statistics) between (1) %diatom and ChlF and (2) %diatom and  $b_{bp}$  would be much simpler than Fig.5c and 5d to latter discussions in subsection 4.1.*

Answer: Following the reviewers suggestions, we have calculated the suggested statistics. Calculated values are now part of the text in the same paragraph where we discuss figure 5: “Changes in Chl F or  $b_{bp}$  were not strongly correlated with variability of % diatom<sub>C</sub> (respective  $r^2$  of 0.21 and 0.16, and p of <0.01 and p<0.1).”

Opposite to reviewer, we believe that figure 5 is of grave importance to the Reader’s understanding of the paper. The point of Fig. 5C is to show that, while there is considerable scatter, that the chlorophyll-to-cell carbon ratio is greater when diatoms dominate. The point of Fig. 5D is to show that changes in the percentage of heterotrophic carbon to total carbon is not driving the optical index. The ratio is driven by the changes in the phytoplankton composition.

### *Subsection 3.4*

L4-8 in P12847: Do you mean score instead of loading here?

Answer: To make the figure caption clearer, we have changed the figure caption to read: “The length of a single parameter vector (black line with arrow) describes its contribution to the PC,…”

L9: I can't see, from the information in Fig. 7, (1) that PC 2 shows no significant difference in the % diatom\_c product among stations for the two types of diatom communities, i.e. Group 2 and 3” and (2) that PC1 can separate them as a function of nutrient concentrations, since which data points (stations) correspond to what group is not shown in the figure.

Answer: It seems that the misunderstanding here arises from the fact that it was not clearly defined that color coding represents the association of certain stations with a specific group (as defined by the optical index). We have rewritten the figure caption, so it clearly states which color is associated with which group:

“PCA biplot for R/V Knorr CTD stations (n = 38), color coded by median Chl F/  $b_{bp}$  for 10-50 m, where blue to Group 1, yellow to Group 2 and red to Group 3.”

Subsection 4.1 L9-12: Would the author please explain, step by step, why they refer to “relationship between POC and  $b_{bp}$  as a function of plankton community composition” here, rather than a relationship between  $b_{bp}$  and the community composition? I guess the latter makes more sense in the present context here. Since the authors have measurements of  $b_{bp}$  and %diatom, they should be able to check by their own measurements whether or not  $b_{bp}$  varies with plankton community composition (see also my comment for subsection 3.3). If  $b_{bp}$  does NOT have correlation with community structure, the authors may want to look at a relationship between ChlF and %diatom (e.g. scatter plot) to check if ChlF alone is correlated to %diatom (i.e. ChlF alone is sufficient to explain %diatom), especially when the authors believe that effects of solar quenching and nutrient limitations on ChlF are minor or minimized in their dataset (L4-L6, P12849). The authors may also want to explain (i) what is an advantage(s) to normalize ChlF by  $b_{bp}$  as an optical index for %diatom and (ii) whether the normalization actually enhance a signal of community composition, or weaken the signal, especially if  $b_{bp}$  have correlation with community structure. I made comments above, because a comparison between ratios is sometimes not straightforward since numerator (or denominator) of a ratio is not a direct translation of that of another ratio, even though they may have a certain degree of correlation.

Answer: Figure 4A shows that values of chlorophyll fluorescence alone cannot explain the difference in community composition; for the same values of Chl F,  $b_{bp}$  varies by a factor of 2.

We discuss this above, but repeat here for convenience.

Section 4.1 asks the question “Why does the  $Chl F/b_{bp}$  ratio vary?” and systematically eliminates potential competing explanations for the variability in the ratio:

- 1) We reject fluorescence non-photochemical quenching as a source of the variability, as all data from depths shallower than 10 meters are rejected. Figure 2C shows the relationship between fluorescence and light; quenched data are excluded. Nutrient limitation, apart from Si limitation, is not a potential source of variability; nitrate is in great excess ( $> 8 \mu\text{M}$ ) at this time of year. Although phosphate was not measured, no report from the subpolar North Atlantic has ever implicated this nutrient as a limiting nutrient. Hence we reject physiology as the explanation for the difference in the  $Chl F/b_{bp}$  ratio.
- 2) Other field studies show higher  $Chl$ -to-carbon ratios for diatom dominated communities in contrast to communities dominated by small phytoplankton (Llewellyn et al., 2005; Putland and Iverson, 2007; Li et al., 2010).
- 3) While it could be possible that the ratio changed because heterotrophic protists became more abundant, Fig. 5D shows that changes in the percentage of heterotrophic carbon to total carbon is not driving the optical index.

We conclude – if chlorophyll fluorescence is a proxy for chlorophyll concentration (please see Fig. 2) and that if optical backscatter is a proxy for particulate organic carbon (Cetinić et al, 2012) – that higher diatom chlorophyll-to-carbon ratios are responsible for the observed higher  $Chl F/b_{bp}$  ratios.

Following the reviewers suggestions, we have calculated the suggested statistics. Calculated values are now part of the text in the same paragraph where we discuss figure 5: “Changes in  $Chl F$  or  $b_{bp}$  were not strongly correlated with variability of % diatom<sub>C</sub> (respective  $r^2$  of 0.21 and 0.16, and  $p$  of  $<0.01$  and  $p<0.1$ ).”

In our Conclusions we make a very important cautionary statement: “The interpretation of these ratios must be based on *in situ* validation and used within a limited set of conditions, at least until a better mechanistic understanding is developed.” We believe that we have done a very thorough job of *in situ* validation, which then allows us to make a statement about the spatial and temporal variability of the phytoplankton communities.

*L13: “making a change in particle optics an unlikely explanations” Don’t particle size and refractive index vary with particle concentration in natural environment? (In other words, there is no correlation among them?)*

Answer: We are trying to say that regardless of the community composition, relationships between  $b_{bp}$  and POC remained constant in this environment. Cetinić et al. (2012) discusses in detail how the change in community composition and associated changes in morphology, size and refractive index did not affect the dominant drivers of POC/ $b_{bp}$

relationships. Later in the season, when coccolithophores bloom in the system, the POC/ $b_{bp}$  relationship again changes as a function of plankton composition, due to the increased coccolithophorid backscattering (Alkire et al., 2014). In our Conclusions we now clearly state: “The interpretation of these ratios must be based on *in situ* validation and used within a limited set of conditions, at least until a better mechanistic understanding is developed.”

*Subsection 4.2 The author found that Si-limitation is associated to “highest values” of the optical index. While this is a good finding, can the authors give a quantitative guidance on how “high” the values should be to imply Si-limitation, because I am currently unsure how this finding can actually be useful for users of the authors’ science.*

Answer: In subsection 3.2, last paragraph (in original discussion paper page 12845, L6 – 16) quantitative definitions of each of the groups were provided. Unfortunately, there is no hard and fast rule to diagnose Si-limitation vs. non-limitation. Figure 4B shows a continuum for Group 3 (Si-limited diatoms), with excess fluorescence likely increasing as Si limitation became more pronounced. Since relatively few studies report chlorophyll fluorescence as a function of Si limitation, please see Cleveland and Perry (1987) for a simple but useful discussion of excess fluorescence for nitrogen limitation.

*Subsection 4.3 I am not sure if this section (hence, Fig.9 also) is needed, since no significant conclusion was drawn from here, as the authors admit it by stating “our analysis did not manage to resolve the primary drivers of the observed spatial patchiness” in Conclusion section. If patchiness were to be discussed, more extensive analysis would be needed to draw a conclusion. In any case, discussions of patchiness without a significant conclusion distract a story of the manuscript.*

Answer: See answer above, third major point. Repeated here for convenience:

However, we do not agree with the reviewer that our analysis of patchiness is not important and distracting. This is, to our knowledge, first analysis of this kind, where distribution of the phytoplankton community was assessed on such high spatial and temporal resolution. Without the patchiness study, this is just a methods paper. In the manuscript, we have alluded that spatial patchiness is associated with physical processes that were happening on the larger scale, and pointed to models that have demonstrated that such patchiness, in these types of systems, originates from mostly physical drivers. Our analysis did not manage to resolve the primary drivers of the patchiness primarily due to the sampling scheme; hence, we could not resolve temporal from spatial variability. Secondly, due to the lack of instruments for measuring higher trophic levels (zooplankton) on the same scales, we cannot say anything about potential top-down

control of this spatial patchiness. Here, we are presenting a methodology that could, in the future, in combination with different sampling schemes and a new generation of imaging/acoustic instruments, offer a better view into the forcing functions that lead to heterogeneity of oceanic biodiversity and associated biogeochemistry.

*Section 5 The authors should include their conclusion such as (1) Chl/C ratio is responsible for ChlF/bbp and (2) the highest values of ChlF/bbp is an indicative of Si-Limitation to diatom, since they are keys to interpret how the optical index the authors propose works.*

Answer: See answer above, first major point. Repeated here for convenience:

Changes have been made in Title, Abstract and Conclusion to point out to these results more clearly.

In the Abstract, we added the following sentence:

“Observed changes in optical index were driven by taxa-specific chlorophyll-to-autotrophic carbon ratios and by physiological changes in *Chl F* driven by the silica limitation.”

In the Conclusions we have added and modified text to the following:

The observed shift in the optical index was primarily driven by the change in phytoplankton composition and distribution of biomass, reflecting differences in taxa-specific chlorophyll-to-autotrophic carbon ratios Furthermore, the optical index allowed us to observe changes in the physiological status of the community as well, clearly isolating the senescent, Si-limited, termination stage of the diatom bloom from surrounding patches of diatoms not yet in senescence.

*Fig. 3 Please increase a font size. Please describe what DM, E, S, M, Ed and P means in figure caption, too.*

Answer: This figure will, in final version of the paper, be such that the font size is the same as in all other figures; currently, due to the format of the BGD, font seems smaller. Definition of the symbols is now part of the caption; Section 3.1 references the origin of these symbols (i.e., Alkire et al., 2012).

*Fig.6 Please consider merging Fig. 6 into Fig. 3*

Answer: We believe the current order of presentation of material aligns with the text. However, we have now added a reference to the end of the Fig. 3 caption: “Also see Fig. 6.”

References:

Alkire, M. B., et al. (2014). Net community production and export from Seaglider measurements in the North Atlantic after the spring bloom, *J. Geophys. Res.*, 119, 6121-6139.

Cetinić, I., Perry, M. J., Briggs, N. T., Kallin, E., D'Asaro, E. A., and Lee, C. M. (2012). Particulate organic carbon and inherent optical properties during 2008 North Atlantic Bloom Experiment, *J. Geophys. Res.*, 117, C06028, 10.1029/2011jc007771.

Cleveland, J., and Perry, M. Quantum yield, relative specific absorption and fluorescence in nitrogen-limited *Chaetoceros gracilis*, *Marine Biology*, 94, 489-497.



1 A simple optical community index to assess shows spatial  
2 and temporal heterogeneity in plankton community  
3 composition spatial patchiness during the 2008 North  
4 Atlantic Bloom

5  
6 I. Cetinić<sup>1</sup>, M. J. Perry<sup>1</sup>, E. D'Asaro<sup>2</sup>, N. Briggs<sup>1</sup>, N. Poulton<sup>3</sup>, M. E. Sieracki<sup>3, \*</sup> and  
7 C. M. Lee<sup>2</sup>

8 [1]{Ira C. Darling Marine Center, School of Marine Sciences, University of Maine, Walpole,  
9 Maine, USA}

10 [2]{Applied Physics Laboratory and School of Oceanography, University of Washington,  
11 Seattle, Washington, USA}

12 [3]{Bigelow Institute for Ocean Sciences, East Boothbay, Maine, USA}

13 [\*]{now at: National Science Foundation, Arlington, VA, USA }

14 Correspondence to: I. Cetinić (iceticnic@gmail.com)

15  
16 **Abstract**

17 The ratio of two *in situ* optical measurements, chlorophyll fluorescence (*Chl F*) and optical  
18 particulate backscattering ( $b_{bp}$ ), varied with changes in phytoplankton community composition  
19 during the North Atlantic Bloom experiment in the Iceland Basin in 2008. Using ship-based  
20 measurements of *Chl F*,  $b_{bp}$ , chlorophyll *a* (*Chl*), HPLC pigments, phytoplankton composition  
21 and carbon biomass, we found that oscillations in the ratio varied with changes in plankton  
22 community composition; hence we refer to *Chl F*/ $b_{bp}$  as an “optical community index”. The  
23 index varied by more than a factor of two, with low values associated with pico- and  
24 nanophytoplankton and high values associated with diatom dominated phytoplankton  
25 communities. Observed changes in optical index were driven by taxa-specific chlorophyll-to-  
26 autotrophic carbon ratios and by physiological changes in *Chl F* driven by the silica limitation.  
27 Observed changes in optical index were driven by the taxa specific chlorophyll to autotrophic

1 | ~~carbon ratios and physiological changes in *Chl F* driven by the silica limitation.~~ A Lagrangian  
2 | mixed-layer float and four Seagliders, operating continuously for two months, made similar  
3 | measurements of the optical community index and followed the evolution and later demise of the  
4 | diatom spring bloom. Temporal changes in optical community index and, by implication the  
5 | transition in community composition from diatom to post-diatom bloom communities, were not  
6 | simultaneous over the spatial domain surveyed by the ship, float and gliders. ~~Not only~~  
7 | ~~phytoplankton biomass, but also community composition was patchy at the submesoscale.~~ The  
8 | ratio of simple optical properties measured from autonomous platforms, when carefully  
9 | validated, provides a tool for studying phytoplankton patchiness on extended temporal scales and  
10 | ecologically relevant spatial scales, and should offer new insights into the processes regulating  
11 | patchiness.

12

## 13 | 1 Introduction

14 | Autonomous observations of phytoplankton are becoming increasingly ubiquitous, including *in-*  
15 | *situ* ~~remote~~ optical sensing from Argo-type and Lagrangian floats, gliders, and moorings, as well  
16 | as remote sensing from space. Phytoplankton biomass is assessed through several different  
17 | optical proxies including *in situ* chlorophyll *a* fluorescence (*Chl F*; Lorenzen, 1966),  
18 | phytoplankton absorption coefficient ( $a_{phy}(\lambda)$ ) or particulate absorption coefficient in waters  
19 | dominated by phytoplankton (Bricaud et al., 1995; Roesler and Barnard, 2014), and chlorophyll  
20 | derived from *in situ* or remotely-sensed ocean reflectance at visible wavelengths (O'Reilly et al.,  
21 | 1998). High-frequency optical measurements are ideal for detecting temporal change and spatial  
22 | patchiness, and in improving understanding of the role of meso- and submeso-scale physics on  
23 | the distribution of phytoplankton in the ocean (Denman and Platt, 1976; Yoder et al., 1987;  
24 | Munk, 2000). Autonomous optical observations have enabled advances in understanding the  
25 | timing of and mechanisms responsible for initiating blooms (Perry et al., 2008; Boss and  
26 | Behrenfeld, 2010; Ryan et al., 2011; Mahadevan et al., 2012; Matrai et al., 2013).

27 | Less common, more challenging, but increasingly important are autonomous measurements of  
28 | phytoplankton community composition. Knowledge of the community composition is critical to  
29 | understanding and predicting vital ecosystem functions such as carbon flux and efficiency of  
30 | carbon transfer to higher trophic levels (biomass is not enough), particularly as the oceans

1 change in response to climate change and ocean acidification. A few direct autonomous  
2 measurements of phytoplankton community composition have been made, but only on moorings  
3 due to the high power consumption of the flow or imaging-in-flow cytometric sensors (Olson  
4 and Sosik, 2007; Sosik and Olson, 2007; Campbell et al., 2013). A diversity of satellite-based  
5 algorithms for determining phytoplankton functional types from ocean color reflectance has been  
6 developed in the last decade (see review of Moisan et al., 2012), although without community  
7 consensus as to robustness. Nencioli et al. (2010) implied that changes in the ratio of *Chl*-to-  
8 particulate beam attenuation coefficient ( $c_p$ ) and the backscattering ratio ( $b_{bp}/b_p$ , where  $b_{bp}$  is total  
9 particulate scattering coefficient and  $b_p$  is backscattering coefficient) are associated with changes  
10 in phytoplankton composition and physiological (light) adaptation in eddies off Hawaii. In a  
11 mooring study of the spring bloom in the Labrador Sea, change in phytoplankton species  
12 composition is offered as the explanation for the observed variability in  $Chl F/c_p$ , although this  
13 suggestion is unconfirmed by *in situ* measurement of species composition (Strutton et al., 2011).

14 In this study we define an “optical community index” as the ratio  $Chl F$ -to- $b_{bp}$  and connect it to  
15 plankton community composition using ship-based measurements of  $Chl F$ ,  $b_{bp}$ , HPLC pigments,  
16 phytoplankton composition, and carbon biomass during two cruises to the Iceland Basin. For two  
17 months during the 2008 North Atlantic Bloom experiment (NAB 2008), we used a Lagrangian  
18 float as the reference frame to track the initiation of the diatom bloom in mid-April, through  
19 depletion of silicic acid and bloom termination in mid-May. The optical index,  $Chl F/b_{bp}$ , varied  
20 as a function of plankton community composition, decreasing by a factor of two as the early  
21 diatom spring bloom community transitioned into a recycling community dominated by smaller  
22 pico- and nanophytoplankton (Cetinić et al., 2012). Rigorous cross-calibration of optical sensors  
23 amongst all platforms enabled us to project the optical community index to data collected by four  
24 Seagliders to construct a spatial time series of the evolution of phytoplankton community  
25 structure and to document its spatial heterogeneity. This approach, of using simple optical  
26 measurements validated with more expensive ship-based measurements, allows projection of the  
27 ship measurements to broader temporal and spatial scales.

28

## 1 2 Material and methods

### 2 2.1 Study site and platforms

3 A Lagrangian float and four Seagliders were deployed near the JGOFS NABE 60°N site  
4 (Ducklow and Harris, 1993) from the *R/S Bjarni Saemundsson* on yearday, YD, 95 (4 April  
5 2008; Fig. 1; (Briggs et al., 2011; Alkire et al., 2012; Mahadevan et al., 2012). The float tracked  
6 the horizontal motion of the mixed layer for almost two months, until the end of its mission on  
7 YD 146 (25 May 2008). An extensive discussion of the evolution of the bloom in the patch  
8 tracked by the float is provided in Alkire et al. (2012). The gliders were piloted to survey an  
9 approximately 50 km region around the float. Depending on currents and eddies, they  
10 occasionally swept further away (up to 175 km from the float). By the end of the float  
11 deployment in late May, they operated within 50 km of the float. A water sampling and sensor  
12 inter-calibration cruise on the *R/V Knorr* occurred between YD 123 –142 (2 – 21 May 2008),  
13 when the ship surveyed waters in proximity of the float and gliders.

14 The Lagrangian float, designed and built at the University of Washington Applied Physics  
15 Laboratory, was similar to the MLFII model described in D'Asaro (2003). The float's deployment  
16 and sampling strategy, detailed in Alkire et al. (2012), were designed to mimic the motion of  
17 plankton, drifting within the mixed layer; once per day (~ 15 UTC) it profiled from the surface to  
18 a depth of ~ 230 m, returning thereafter to the mixed-layer drift mode. The float measured  
19 temperature and conductivity with two CTD sensors (Sea-Bird Electronics, Inc., SBE 41), one  
20 near the top and another near the bottom of the platform ([see list of measured parameters and](#)  
21 [associated methods in the Table 1](#)). A WET Labs FLNTU mounted at the bottom of the float  
22 measured *Chl F* ( $\lambda_{\text{ex}}=470$  nm,  $\lambda_{\text{em}}=700$  nm) and optical backscattering ( $\lambda=700$  nm) at an angle,  $\theta$ ,  
23 of 140°. Photosynthetically active radiation, PAR (400 – 700 nm), was measured by a  
24 downwelling cosine PAR sensor (LI-COR 192-SA) mounted at the top of the float.

25 Seagliders, autonomous underwater vehicles designed for long ocean deployments, move  
26 forward horizontally while gliding vertically in a sawtooth pattern (Eriksen et al., 2001). Four  
27 Seagliders (SG140, SG141, SG142 and SG143) were deployed during this experiment, with an  
28 adaptive mission to follow the Lagrangian float on its path and provide measurements on larger  
29 spatial scales and to depths of 1,000 m. All gliders were equipped with an unpumped custom  
30 Sea-Bird Electronics, Inc., CT sensor that measured conductivity and temperature and carried a

1 WET Labs BB2F that measured backscattering at two wavelengths (470 and 700 nm;  $\theta=124^\circ$ )  
2 and *Chl F* ( $\lambda_{\text{ex}}=470$  nm,  $\lambda_{\text{em}}=700$  nm).

3 Extensive surveys around the float and glider deployment area were carried out during a three-  
4 week process cruise aboard the *R/V Knorr*, with 134 CTD profiles. The CTD rosette was  
5 equipped with a Sea-Bird Electronics, Inc., SBE 911*plus* CTD. A WET Labs FLNTU (similar to  
6 that on the float) was mounted on the bottom of the frame. A Biospherical QSP2300 sensor  
7 mounted on the top of the CTD rosette frame measured scalar underwater PAR. The same set of  
8 optical sensors was used during the short, six-day deployment cruise aboard the *R/S Bjarni*  
9 *Saemundsson*; fewer profiles and samples were collected during this cruise (9 CTD profiles).

10 All data used in this paper and the cited calibration reports are available under the project name  
11 NAB 2008 from the Biological and Chemical Oceanography Data Management Office (BCO-  
12 DMO, at <http://osprey.bcodmo.org/project.cfm?flag=view&id=102&sortby=project>).

## 13 **2.2 In situ optical measurements and sensor inter-calibration procedure**

14 *Chl F* and  $b_{bp}$  were measured on the float, four gliders and ship, with a total of six sensors (two  
15 FLNTUs and four BB2Fs). The ship's FLNTU was used as the primary reference sensor to  
16 which the autonomous sensors were brought into alignment via *in situ* inter-calibrations. All  
17 sensors were factory calibrated before and after the cruise *en masse* (with the exception of  
18 sensors on SG142, which was not retrieved). Dark readings (voltage) for both channels of the  
19 ship's FLNTU sensor were measured *in situ* by covering the detector window with black  
20 electrical tape on two profiles to 600 m, as suggested by Twardowski et al. (2007); these *in situ*  
21 dark measurements agreed with the mean factory dark volts. Prior to inter-calibration, mean pre-  
22 and post-deployment factory calibrations were applied to all sensors to convert *Chl F* into  
23 nominal *Chl* concentration and scattering measurements to the volume scattering function,  $\beta_{total}$   
24 ( $\theta$ , 700 nm), which was converted to  $b_{bp}$  as follows. The volume scattering function of seawater,  
25  $\beta_{sw}(\theta$ , 700 nm), calculated following Zhang et al. (2009), was subtracted from  $\beta_{total}(\theta$ , 700 nm) to  
26 yield the volume scattering function of particles,  $\beta_p(\theta$ , 700 nm), which was then converted to  $b_{bp}$   
27 by multiplying  $\beta_p(\theta$ , 700 nm) by  $2\pi\chi$ , using  $\chi$  factors of 1.132 for FLNTU and 1.077 for BB2F  
28 (Sullivan et al., 2013).

1 Offsets were applied to the factory calibrated glider data to bring the pre-bloom deep values for  
2 all gliders into alignment. The autonomous sensors were further aligned with ship sensors using  
3 matchups from intentional calibration stations, in which the float or glider was brought to the  
4 surface within close proximity to the ship and a CTD cast made as the vehicle descended. A total  
5 of 11 float casts and 2-3 casts per glider were made. Profiles were aligned in density coordinate  
6 space and ship profiles were interpolated to match the densities of the more sparse autonomous  
7 measurements, creating a ship-autonomous sensor matchup for every autonomous measurement  
8 from each of the inter-calibration casts. Matchups from float inter-calibration casts were pooled  
9 to calculate a single linear regression for each sensor type (*Chl F* and  $b_{bp}$ ), which were used to  
10 align float sensors to the ship. Matchups were insufficient to align each glider to the ship  
11 independently, so matchups from all four gliders (already aligned at depth) were pooled to  
12 calculate a single regression per sensor type, aligning all gliders with the ship as well. Finally,  
13 *Chl F* for all sensors was converted to volts,  $V_5$  (referenced to the ship's FLNTU). More details  
14 on the inter-calibration procedures are available in (Briggs et al., 2011) and in the reports  
15 available on BCO-DMO (Briggs, 2011).

16 PAR was measured with a LI-COR cosine PAR on the float and a Biospherical scalar PAR on  
17 the ship's CTD Rosette frame. Both instruments were factory calibrated prior to the experiment,  
18 with NIST traceable calibration lamps; the data reported here are based on factory calibrations  
19 only. The float made a single daily vertical profile (~ noon/early afternoon); PAR from this  
20 profile was used to derive the diffuse attenuation coefficient,  $K_D$ , using all data  $> 10 \mu\text{mol}$   
21  $\text{photons m}^{-2} \text{s}^{-1}$ .  $K_D$  was applied to all measurements of PAR acquired during the float's mixed-  
22 layer drift mode and extrapolated to the surface to produce hourly subsurface PAR fields from  
23 which daily isolumes were computed. The isolume of  $0.415 \text{ mol photons m}^{-2} \text{ d}^{-1}$  is taken as the  
24 radiation level below which net photosynthesis does not occur (Letelier et al., 2004; Boss and  
25 Behrenfeld, 2010), and is hereafter referred to as the 0.415 isolume.

### 26 **2.3 Water samples and laboratory analyses**

27 Water samples were collected from the CTD upcast with 10 L Niskin bottles mounted on the  
28 CTD Rosette. Samples for nitrate plus nitrite, hereafter referred as to nitrate, and silicic acid, Si,  
29 were collected directly from Niskin bottles into acid-washed LDPE bottles, pre-rinsed three  
30 times with sample (Kallin et al., 2011). Unfiltered water samples were frozen immediately after

1 collection and stored at -20° C for up to 8 mo. Samples were thawed in the dark prior to analysis  
2 and vigorously vortexed (Gordon et al., 1992) prior to absorptiometric analysis on a Lachat  
3 Quickchem 8000 Flow Injection Analysis System (Lachat, 1996, 1999). In addition to quality  
4 control of the Lachat output spectra, profiles of Si and nitrate concentrations were examined  
5 following the recommendation of the IODE workshop on quality control of chemical  
6 oceanographic data (IOC, 2010).

7 Water samples for pigments and spectral absorption coefficients were filtered through Whatman  
8 GF/F filters. Samples for fluorometric analysis of *Chl* were extracted in 5 mL of 90% acetone at  
9 -20° C for 24 h and analyzed on a Turner Designs Model 10-AU digital fluorometer that was  
10 calibrated before and after the field experiment with Turner Designs *Chl* standards. *Chl*  
11 concentrations were calculated following JGOFS protocol (Knap et al., 1996). Filters collected  
12 for HPLC pigment analysis were stored in liquid nitrogen until analysis (up to 5 mo). Horn Point  
13 Laboratories performed HPLC pigment analyses, using a methanol-based reversed-phase  
14 gradient C8 chromatography column system and appropriate standards (Van Heukelem and  
15 Thomas, 2001; Hooker et al., 2009).  $Chl_{HPLC}$  is the sum of *Chl* plus chlorophyllide *a*, with the  
16 latter adjusted to *Chl* equivalent mass (x 893.5/614 molecular mass ratio); the ratio of  
17 chlorophyllide-to- $Chl_{HPLC}$  is also reported in *Chl* mass equivalents. Filters collected for  
18 particulate spectral absorption coefficients were scanned at sea on a Varian Cary 50 UV-Visible  
19 spectrophotometer with a xenon flash lamp and a 1.5 nm slit width, following the Mitchell and  
20 Kiefer (1988) method. The filters were extracted in hot methanol and re-scanned to measure  
21 residual detrital particulate absorption (Kishino et al., 1985). The difference between the total  
22 particulate and detrital absorption coefficients was attributed to the phytoplankton absorption  
23 coefficient ( $a_{phy}(\lambda)$ ).

24 Microbial plankton cell size and numerical concentrations were determined on fresh samples at  
25 sea during the May cruise (Sieracki and Poulton, 2011). Cells smaller than 20  $\mu$ m were analyzed  
26 with a flow cytometer (FACScan, BD Biosciences), using *Chl* and phycoerythrin fluorescence as  
27 discriminators for three groups of phytoplankton: eukaryotic pico- and nanophytoplankton,  
28 cryptophytes, and prokaryotic *Synechococcus spp.* (*Prochlorococcus* was not observed).  
29 Heterotrophic microbes were analyzed on separate subsamples and detected using fluorescent  
30 stains; heterotrophic bacteria were stained with PicoGreen – Life Technologies Inc. (Veldhuis et  
31 al., 1997) and heterotrophic nanoprotists were stained with LysoTracker Green – Life

1 Technologies Inc. (Rose et al., 2004). Cell size for all these groups was determined from forward  
2 scatter, where size and scatter relationships were established with microbead size standards and  
3 algal cultures of known cell size (Sieracki and Poulton, 2011). Phytoplankton cell carbon was  
4 estimated from cell size following the algorithm of Verity et al. (1992). Cells larger than 20  $\mu\text{m}$   
5 were analyzed using a Fluid Imaging Technologies FlowCAM, with image collection triggered  
6 by *Chl F*. Four major sub-groups were identified: diatoms, dinoflagellates (autotrophic and  
7 mixotrophic), ciliates, and ‘other’ microphytoplankton. Biovolume estimates were determined  
8 following the method of Sieracki et al. (1989), where particle boundary points were found using  
9 the Connected Component Labeling algorithm of Chang et al. (2004), as implemented in Burger  
10 and Berge (2008). Cell carbon was calculated from derived biovolumes using the algorithms of  
11 Menden-Deuer and Lessard (2000). Heterotrophic microprotists were not enumerated with the  
12 FlowCAM, and hence estimates of their carbon biomass missing from analyses of heterotrophic  
13 carbon. Total particulate organic carbon (POC) was analyzed as reported in (Cetinić et al., 2012).

#### 14 **2.4 Data analysis and derivation of proxies**

15 Optical data were median filtered (7 point running median) to remove spikes associated with  
16 aggregates and other larger particles in the water column (Briggs et al., 2011). Water samples  
17 were collected on the upcast, with the CTD held at a constant depth for 60 s before the Niskin  
18 bottle closed; only data recorded during the last 30 s before bottle closure were used for analysis.  
19 *Chl* samples collected during the *R/V Knorr* cruise were used to convert the ship’s FLNTU *Chl F*  
20 voltage to *Chl* ( $\mu\text{g L}^{-1}$ ) using a non-linear best-fit function of temperature, PAR, depth and YD  
21 (Figs. 2A, B;  $n=835$ ; D’Asaro, 2011); this algorithm mostly removed the effects of solar  
22 quenching (Fig. 2C) and Si limitation (Section 3.4) on *Chl F*. The resulting *Chl* product  
23 converted *Chl F* to *Chl* within an error of 30 – 50% (Figs. 2A, B). This uncertainty, and the lack  
24 of PAR sensors on the gliders, caused us to use *Chl F* rather than *Chl* in the subsequent analysis.  
25 Glider *Chl F* in digital counts was converted to V, referenced to the ship’s FLNTU, based on the  
26 inter-calibration procedures; *Chl F* is therefore reported as V for all platforms and the optical  
27 community index,  $Chl F/b_{bp}$ , is reported in units of V m.

28 In this paper, we focus on properties of the upper water column, i.e., 50 m and shallower.  
29 Daytime fluorescence quenching is a ubiquitous phenomenon in surface layers of the ocean, with  
30 decreases in *Chl F* caused by photo-inhibitory and/or energy-dependent quenching (Sackmann et



1 al., 2008). *Chl F* normalized to fluorometrically measured *Chl* declined at values of PAR > 100  
2  $\mu\text{mol photon m}^{-2} \text{ s}^{-1}$  (Fig. 2C). Since 92 % of all PAR values > 100  $\mu\text{mol photon m}^{-2} \text{ s}^{-1}$  were  
3 measured within the top 10 m by both ship and float, we omitted *Chl F* and  $b_{bp}$  data collected at  
4 depths shallower than 10 m from further analysis for all platforms to avoid potential bias  
5 associated with solar quenching of *Chl F*. However, data from water samples (nutrients, HPLC  
6 pigments, etc.) collected at all depths shallower than 50 m are included in the analyses.

7 Principal component analysis (PCA) for assessing potential sources of variability in *Chl F/b\_{bp}*  
8 was performed on data from 38 CTD profiles from the May cruise. Input parameters for PCA  
9 were temperature, mixed layer depth (calculated as the depth at which density differed from the  
10 mean density in the top 10 m by  $< 0.05 \text{ kg m}^{-3}$ ), depth of the 0.415 isolume, nitrate, Si, *Chl F/b\_{bp}*  
11 and a term representing diatom dominance of phytoplankton biomass (defined in Section 3.3). A  
12 single median value for the upper 50 m was assigned to each parameter for each profile, except  
13 for *Chl F/b\_{bp}* for which median values were calculated for 10 – 50 m (as explained above). The  
14 0.415 isolume for a given day was derived from float data and assigned to a CTD profile based  
15 on YD. Prior to analysis, data were standardized by subtracting the mean and dividing by the  
16 standard deviation. Scores of individual data points were scaled by the maximal absolute value  
17 of the sample scores and maximal coefficient vector length (Matlab code *biplot.m*).

18 A “heterogeneity index” for similarity of plankton community composition was calculated based  
19 on similarity/dissimilarity of *Chl F/b\_{bp}* between pairs of autonomous platforms. The six-hour  
20 median value of *Chl F/b\_{bp}* between 10 and 50 m was determined for each platform and assigned  
21 to one of three optical community groups (as described in Results). These assignments were then  
22 compared for each platform pair (total of 10 comparisons). A value of 0 was assigned if the  
23 community groups were identical (low heterogeneity) and a value of 1 (high heterogeneity) if  
24 they were different. The final heterogeneity index reported for a given time is the average of the  
25 10 comparisons.

26

## 1 **3 Results**

### 2 **3.1 The evolution of the spring bloom observed from the Lagrangian float**

3 The evolution and community succession of the spring bloom was measured by the Lagrangian  
4 float. Alkire et al. (2012) divided the evolution into six periods based on measured physical and  
5 biogeochemical parameters. The float was deployed into a deep wintertime mixed layer with *Chl*  
6  $< 0.5 \mu\text{g L}^{-1}$  (the period of *Deep Mixing*, Fig. 3A). During the *Early Bloom* (YD 114 – 119) the  
7 mixed layer shoaled from  $> 100$  m to  $\sim 50$  m, approximately the depth of the 0.415 isolume (Fig.  
8 3B); during this period *Chl* exponentially increased to  $\sim 2 \mu\text{g L}^{-1}$ . Surface phytoplankton  
9 concentration was diluted and net growth was slowed by a storm (*Storm*) which deepened the  
10 mixed layer to  $\sim 100$  m between YD 119 and 123, slightly decreasing near-surface *Chl*.  
11 Following the storm, the upper ocean quickly restratified and the mixed layer shoaled above the  
12 0.415 isolume. *Chl* continued to increase during the *Main Bloom* (YD 124 – 134). Beginning  
13 around YD 126, spikes below 200 m in *Chl F* and  $b_{bp}$  were observed in ship and glider data, as  
14 well as in ship  $c_p$  data, indicating the onset of a flux event of sinking diatom aggregates (Briggs  
15 et al., 2011). *Chl* reached a maximal value of  $4.6 \mu\text{g L}^{-1}$  on YD 133 and shortly thereafter  
16 abruptly declined to a quarter of the peak bloom value,  $\sim 1 \mu\text{g L}^{-1}$ , by YD 137. Bloom  
17 termination continued into the *Eddy* period; *Chl* remained relatively unchanged during the *Post*  
18 *Bloom* period and until the end of the float mission on YD 146.

### 19 **3.2 Diel and longer temporal patterns in the optical community index**

20 The optical community index at the location of the float varied over time on both diel and longer  
21 time scales; the observed diel variability was due mostly to *Chl F*, with the peak consistently  
22 occurring around midnight (Fig. 3A, C, D). Similar diel patterns have been previously observed  
23 for both *Chl F* and  $b_{bp}$  (Marra, 1997; Loisel et al., 2011). Although the effects of solar quenching  
24 on daytime values of *Chl F* (Sackmann et al., 2008) were minimized by removing data from the  
25 upper 10 m (Fig. 2C), a small daytime quenching signal remained. The longer term variations in  
26 *Chl F/b\_{bp}* were considerably larger than the diel and, as shown below, were associated either  
27 with shifts in the phytoplankton community composition, i.e., diatom vs. pico and  
28 nanophytoplankton dominance, or a physiological response of diatoms to Si limitation between  
29 YD 133 – 136.

1 During the *Deep Mixing* period, the optical community index was low and variable (Fig. 3D).  
2 Part of this variability may have been due to instrumental noise since both *Chl F* and  $b_{bp}$  were  
3 small (Fig. 3C). There is insufficient ship data during this period to determine whether the  
4 variability was due to real fluctuations in community composition. Starting mid-way into the  
5 *Early Bloom*, the optical community index increased and remained high until the end of the *Main*  
6 *Bloom* period. As Si concentrations measured from ship samples dropped below  $1 \text{ mmol m}^{-3}$   
7 (YD 133 – 136), the optical community index increased to its highest values. It then abruptly  
8 decreased by more than a factor of two (end of *Main Bloom*) and remained low (*Eddy* and *Post*  
9 *Bloom*) through the end of the float mission.

10 Figure 4A shows a scatter plot of *Chl F* vs.  $b_{bp}$ ; three groupings are evident. Within Groups 1 and  
11 2, *Chl F* and  $b_{bp}$  covaried linearly but with different slopes; Group 1:  $Chl F = 53.63 b_{bp} + 0.01$ ;  
12 Group 2:  $Chl F = 105.34 b_{bp} - 0.02$ . The range in  $b_{bp}$  was equivalent, indicating that the  
13 relationship was not driven by the changes in magnitude of  $b_{bp}$ . Group 1 is characteristic of the  
14 *Eddy* and *Post Bloom* periods; Group 2 of the *Early* through *Main Bloom* periods. Groups 2 and  
15 3 reflect a biphasic relationship, with a break in the slope at higher values of  $b_{bp}$ . The regression  
16 intercept for the third group is non-linear and does not pass near zero (regression not shown).  
17 Group 3 occurred only in the latter part of *Main Bloom* period.

18 The frequency histogram in Fig. 4B also illustrates these patterns, with two clearly defined  
19 groupings of the optical community index: low (Group 1 is centered on 58 V m) and  
20 intermediate (Group 2 is centered on 98 V m). Group 3 is more diffuse. As a way to more clearly  
21 separate Groups 2 and 3, a frequency distribution was constructed for YDs 120 – 127, a period  
22 when diatoms were clearly dominant and Si was not limiting. The results of this analysis (shown  
23 as a dashed gray line in Fig. 4B) confirmed the upper limit of the optical community index for  
24 Group 2 as 120 V m. Indices in excess of 120 V m were classified as Group 3. Cetinić et al.  
25 (2012) refers to Group 1 as a ‘recycling community’ comprised primarily of pico- and  
26 nanophytoplankton and Groups 2 and 3 as a ‘diatom community’; in Section 3.3 we present the  
27 justification for these designations, which are used henceforth.

### 3.3 Optical community index is a proxy for phytoplankton community composition

Ship-based measurements of phytoplankton cell carbon allowed us to establish that changes in *Chl F/b<sub>bp</sub>* corresponded to changes in phytoplankton community composition. In May, the fraction of diatom cell carbon as a percentage of total autotrophic cell carbon, % *diatom<sub>C</sub>*, was calculated from flow cytometer and FlowCAM samples. The diatoms were primarily chain formers, belonging to the genera *Chaetoceros*, *Thalassionema* and *Pseudo-nitzschia* (K. Richardson, *pers. comm.*). Coincident measurements of flow cytometer, FlowCAM and HPLC pigments (n=16) were used to create a proxy that converted the mass ratio of fucoxanthin-to-*Chl* (*Fuco/Chl*, g/g) to the fraction of diatom cell carbon. This relationship, shown in Fig. 5A (Type II regression,  $r^2=0.78$ ,  $p<0.01$ ), allowed us to include all HPLC samples in the analysis of community composition:

$$\% \text{ diatom}_C = 77.36(\pm 9.87) \times \text{Fuco/Chl} - 11.31(\pm 4.85). \quad (1)$$

The combined data set, including both the direct % *diatom<sub>C</sub>* measurements and those derived from (1), was designated as % *diatom<sub>C</sub> product* and provided information for a total of 94 individual samples from 42 stations, of which 4 were from early April and 38 from May.

Figure 5B used the % *diatom<sub>C</sub> product* to show that the optical community index was low when pico and nanoplankton dominated (Group 1) and high when diatoms dominated (Groups 2 and 3), with a transition at about 80 V m, as in Figs. 3D and 4B. There was no clear distinction between Groups 2 and 3 in terms of percent diatom domination. An alternative visualization of the optical community index also shows that the highest values were associated with diatoms (Fig. 6A). Changes in *Chl F* or *b<sub>bp</sub>* were not strongly correlated with variability of % *diatom<sub>C</sub>* (respective  $r^2$  of 0.21 and 0.16, and  $p$  of  $<0.01$  and  $p<0.1$ ).

During May, the ratio of *Chl*-to-autotrophic carbon showed a moderate trend of higher ratios associated with diatom-dominated communities (Fig. 5C; Type II regression,  $r^2=0.55$ ,  $p<0.01$ ). Here % *diatom<sub>C</sub>* is used rather than the % *diatom<sub>C</sub> product*, since total autotrophic carbon is available only from flow cytometer and FlowCAM samples. Samples from periods when mixed layers were deeper than 70 m were excluded to avoid confounding effects of low light photo-adaptation on the *Chl*-to-carbon ratio.

1 The absolute magnitude of heterotrophic carbon (sum of heterotrophic bacteria and  
2 nanoflagellate carbon) varied between 15 and 30  $\mu\text{g L}^{-1}$ . The corresponding percentage of  
3 heterotrophic carbon-to-POC varied between  $\sim 10 - 25\%$  and was not correlated with the  
4 variability observed in the optical community index (Fig. 5D,  $n=74$ , Type II regression,  $r^2=0.07$ ,  
5  $p>0.01$ ). Thus, the optical community index  $Chl F/b_{bp}$  varies with the fraction of the planktonic  
6 carbon due to diatoms.

### 7 **3.4 Principal component analysis**

8 PCA of *R/V Knorr* CTD profiles (Fig. 7,  $n=38$ ) also show a separation between recycling and  
9 diatom dominated communities. Principal component one (PC 1; 38.5% of variance) is  
10 dominated by an inverse relationship of surface temperature with mixed layer depth and nutrient  
11 concentrations. However, PC 2, explaining nearly as much of the variance (30.2 %), is nearly  
12 parallel to  $Chl F/b_{bp}$  (i.e., the  $Chl F/b_{bp}$  vector is nearly vertical in Fig. 7). Most stations with a  
13 recycling community (low optical community index) had lower loadings on PC 2, while stations  
14 with a diatom community (high optical community index) had higher loadings. The analysis  
15 confirmed that trends observed in  $Chl F/b_{bp}$  are associated with the proportion of diatoms, as the  
16 % *diatom<sub>C</sub> product* had the largest loading on the second component (0.66).

17 Although PC 2 shows no significant difference in the % *diatom<sub>C</sub> product* among stations for the  
18 two types of diatom communities, i.e., Groups 2 and 3 ( $n=27$ ; two tailed t-test,  $p > 0.05$ ), PC 1  
19 separated them as a function of nutrient concentration, as shown by the high loadings on Si  
20 (0.57). Nitrate was not a limiting factor for phytoplankton growth, decreasing from an initial  
21 concentration of  $> 12 \text{ mmol m}^{-3}$  in early April to a minimal value of  $\sim 8 \text{ mmol m}^{-3}$  in late May  
22 (Alkire et al., 2012). In contrast, Si was likely limiting to diatoms by the peak of the bloom,  
23 decreasing from initial surface concentrations of  $> 4 \text{ mmol m}^{-3}$  in early April to  $< 1 \text{ mmol m}^{-3}$   
24 towards the end of the *R/V Knorr* cruise (Fig. 6B).

### 25 **3.5 Ancillary analyses**

26 Ancillary analyses of chlorophyllide and phytoplankton UV absorption spectra are also  
27 indicative of differences between diatoms vs. pico and nanophytoplankton. The highest ratios of  
28 chlorophyllide-to- $Chl_{\text{HPLC}}$  were measured at CTD stations with high values of  $Chl F/b_{bp}$  (Fig.  
29 8A). Unfortunately, no HPLC samples were collected next to the float during the period when

1 *Chl F/b<sub>bp</sub>* was highest. In May some of the phytoplankton absorption spectra exhibited unusual  
2 spectra. UV peaks with a ratio of  $a_{phy}(\lambda\text{-UV peak})/a_{phy}(676)$  in excess of 2 were correlated with a  
3 high optical index, i.e., in excess of 80 V m (Fig. 8B); 18 out of 63 spectra fit this criterion.  
4 While most UV peaks were centered between 325 – 330 nm, four samples associated with Group  
5 3 had up to seven-fold higher peak heights with maxima shifted to lower wavelengths (310 – 320  
6 nm), increased absorption at 412 nm and reduced absorption at 437 and 467 nm peaks.

### 7 **3.6 Patchiness of phytoplankton communities**

8 The evolution of the diatom spring bloom, its demise and transition to a pico- and  
9 nanophytoplankton community was assessed over a two-month period for the float and four  
10 gliders. Both the optical community index and mixed layer depths showed some spatial  
11 variability (Figs. 9A, B), likely reflecting submesoscale variability as well as variability in the  
12 timing of the diatom bloom initiation and termination. During the bloom peak in May, the *R/V*  
13 *Knorr* carried out a series of bow-tie sampling patterns and the optical community index varied  
14 between some of the lowest and highest values as the ship moved in and out of different patches  
15 (Fig. 6, YD 130 – 135). The period of greatest heterogeneity in phytoplankton community  
16 composition occurred between YD 115 – 137 (Fig. 9C). The strong salinity component in PC 2  
17 (Fig. 7) also reflects this patchiness; the float patch had an anomalously high value of salinity in  
18 addition to a high value of the optical community index.

19

## 20 **4 Discussion**

### 21 **4.1 Why does the *Chl F/b<sub>bp</sub>* ratio vary?**

22 High and low values of the optical community index were correlated with diatom-, and pico- and  
23 nanophytoplankton-dominated communities, respectively (Figs. 5, 6 and 7). The direct  
24 measurement of HPLC pigments and phytoplankton from the flow cytometer and FlowCAM  
25 allowed us to create an optical proxy for phytoplankton community composition for this specific  
26 period and to apply it to glider and float data to assess community composition over a broader  
27 spatial scale (Fig. 9). The question remains, why does this optical index vary as a function of

1 phytoplankton type? Is it strictly taxonomical, or is it based on physiology, or combination of  
2 both?

3 Ratios must be interpreted with caution, as changes could be due either to the numerator,  
4 denominator, or both. *Chl F* is a proxy for *Chl*, but with physiological variability associated with  
5 solar quenching (Sackmann et al., 2008; Roesler and Barnard, 2014) and nutrient stress  
6 (Cleveland and Perry, 1987). However, neither solar quenching nor Si limitation appears to be  
7 responsible for the difference in optical community index between Groups 1 and 2. The  
8 influence of the former was minimized by the deliberate exclusion of depths less than 10 m.  
9 Nitrogen limitation was unlikely, but indications of Si limitation were correlated only with the  
10 highest values of *Chl F*/ $b_{bp}$  (see Section 4.2, and Figs. 6B and 7). The denominator,  $b_{bp}$ , is a  
11 function of particle concentration. Although  $b_{bp}$  is also influenced by particle size and refractive  
12 index (Stramski et al., 2004), the relationship between POC and  $b_{bp}$  within the mixed layer  
13 during the May NAB 2008 cruise did not vary as a function of plankton community composition  
14 (Cetinić et al., 2012), making a change in particle optics an unlikely explanation.

15 We examined two hypotheses for the observed patterns of the optical community index. First, the  
16 relative contribution of heterotrophic carbon to POC and  $b_{bp}$  could vary systematically between  
17 the different communities. If the contribution of heterotrophs was consistently greater for Group  
18 1, *Chl F*/ $b_{bp}$  would be lower. However, heterotrophic (bacteria and nanoprotist) carbon as a  
19 percentage of POC was not correlated with the optical community index (Fig. 5D), making it  
20 unlikely that heterotrophic carbon was responsible for changes in the ratio. Although  
21 heterotrophic protists > 20  $\mu\text{m}$  were not analyzed, their carbon is less than 30% of the  
22 heterotrophic nanoprotist carbon at this time of year (Verity et al., 1993) and inclusion of these  
23 larger protists would not change the observed trend.

24 Second, the *Chl*-to-carbon ratio of diatoms could be larger than that of pico and  
25 nanophytoplankton, thereby increasing *Chl F*/ $b_{bp}$  in the diatom community. In laboratory  
26 cultures for the same irradiance, *Chl* per cell volume scales inversely with cell size (cf. Fujiki  
27 and Taguchi, 2002), resulting in higher *Chl*-to-carbon ratios for larger cells. Field studies where  
28 cell carbon was determined from measurements of cell volume show higher *Chl*-to-carbon ratios  
29 for diatom dominated communities in contrast to communities dominated by small  
30 phytoplankton (Llewellyn et al., 2005; Putland and Iverson, 2007). In the California Current,

1 observations supported by models also find higher *Chl*-to-carbon ratios for diatoms than  
2 picoplankton for similar environmental conditions (Li et al., 2010). Our data revealed the same  
3 trend, approximately a factor of two higher ratios of *Chl*-to-autotrophic carbon for samples  
4 dominated by diatoms, although with considerable scatter (Fig. 5C). We conclude that  
5 differences observed in *Chl F/b<sub>bp</sub>* between Groups 1 and 2 are primarily due to taxa specific  
6 differences in the cellular *Chl*-to-autotrophic carbon ratios and that the optical community index  
7 *Chl F/b<sub>bp</sub>* varies as a function of the fraction of the planktonic carbon due to diatoms. While  
8 changes in the *Chl*-to-carbon ratio of individual species do occur in response to changing light,  
9 nutrient, and temperature conditions (e.g. Geider, 1987), species succession offers an alternative  
10 hypothesis to that of physiological change as the sole explanation for change in phytoplankton  
11 *Chl*-to-carbon and hence ratios of *Chl F/b<sub>bp</sub>* in the field (cf. Behrenfeld et al. 2005).

## 12 **4.2 Evidence of Si limitation**

13 Analysis by Egge and Aksnes (1992) indicates that diatoms are unlikely to do well in waters with  
14 Si concentrations  $< 2 \text{ mmol m}^{-3}$ . In their review of silicon metabolism in diatoms, Martin-  
15 Jezequel et al. (2000) compiled data for the Michaelis-~~Menton~~-Menten half saturation constant  
16 for Si-dependent growth rate; the median half saturation constant for 17 studies was  $1.0 \text{ mmol m}^{-3}$ .  
17 Concentrations of Si at highest values of *Chl F/b<sub>bp</sub>* were  $< 1 \text{ mmol m}^{-3}$  (Fig. 6B), leading us to  
18 suggest that Group 3 represented diatoms whose photosynthetic physiology was limited by Si.

19 Does Si limitation affect photosynthetic efficiency and *Chl F*? Reduced photosynthetic  
20 efficiency is a typical response to limitation by nitrogen, phosphorous and iron due to the  
21 structural and functional roles of these elements in photosynthesis. For most species, *Chl*  
22 concentration per cell volume decreases with nutrient limitation, while fluorescence normalized  
23 to *Chl* concentration increases when nutrients are limiting (Kruskopf and Flynn, 2006). The  
24 increase in fluorescence is due in part to an increase in the *Chl*-specific absorption coefficient  
25 due to reduced pigmentation and in part to reduced photochemical quenching due to nutrient  
26 limitation (Cleveland and Perry, 1987). While Si itself is not directly associated with  
27 photosynthesis and relatively few papers report the effect of Si limitation on fluorescence  
28 efficiency in diatoms, the available results suggest that Si limitation does reduce photosynthetic  
29 efficiency. For Si-limited cultures of the diatom *Thalassiosira weissflogii*, (Lippemeier et al.,  
30 1999; Bucciarelli and Sunda, 2003) report a decrease in photosynthetic efficiency (equivalent to



1  $F_v/F_m$ ). In a field study in the Iceland Basin and Rockall Trough in May and June 2001, Moore et  
2 al. (2005) found  $F_v/F_m$  to be correlated with Si concentration, suggesting reduction in  
3 photosynthetic capacity in response to Si stress (note, N concentrations in that study were always  
4  $> 3 \mu\text{M}$ , but Si concentrations were often  $< 1 \mu\text{M}$ ). They also found  $\sim 2 \times$  higher values of  $F_0/Chl$   
5 associated with low Si concentrations. During the *Main Bloom* period in NAB 2008, enhanced  
6  $Chl F$  normalized to both  $b_{bp}$  (i.e., optical community index) and extracted  $Chl$  coincided with Si  
7 depletion (Figs. 2D, 4A, 6B, 7). ~~Increase in optical community index was outside of standard~~  
8 During this period Briggs and Gudmundsson (*pers. comm.*) found that rates of net primary  
9 productivity based on float diel cycles of optics and oxygen could only be reconciled with  
10 photosynthesis vs. irradiance (P–E)-based estimates of productivity if the P–E parameters were  
11 reduced with a Michaelis–~~Menton~~Menten-like function and a  $K_s$  of  $1 \mu\text{M}$ . Hence, we propose  
12 that the highest values of  $Chl F/b_{bp}$  are indicative of diatom Si limitation.

13 Two other measurements are also suggestive of physiological effects of Si limitation at the end  
14 of the diatom bloom. Chlorophyllide is a pigment linked with diatom senescence (Lorenzen,  
15 1967; Jeffrey, 1980; Llewellyn et al., 2008). Although chlorophyllide is noted as a potential  
16 extraction artifact (Jeffrey and Hallegraeff, 1987), this pigment has often been used as a marker  
17 for senescent diatoms at the end of diatom blooms in coastal, open ocean, and high latitude  
18 environments (Ridout and Morris, 1985; Head and Horne, 1993; Sigleo et al., 2000; Llewellyn et  
19 al., 2008). High relative concentrations of chlorophyllide were associated with both Groups 2  
20 and 3, suggesting that diatoms were in transition to senescence. Unusual features in  
21 phytoplankton absorption spectra were only found for samples with high optical community  
22 indices, including peaks in the UV typically suggestion of MAAs (mycosporine-like amino  
23 acids; Fig. 8B). While such UV peaks are often interpreted as MAAs, Llewellyn and Airs (2010)  
24 caution that for diatoms, UV absorption peaks can be associated with derivatives of  
25 photosynthetic pigments. Since no direct chemical analyses of MAAs were made, the UV peaks  
26 may be another indicator of diatom senescence. *In toto*, these observations suggest that as Si  
27 became limiting to diatoms, Si limitation was responsible for the highest values of  $Chl F/b_{bp}$ , as  
28 well as the termination of the Main Bloom, leading to subsequent dominance of pico- and  
29 nanophytoplankton that do not require Si in the post-bloom community

### 1    **4.3 Patchiness of phytoplankton communities**

2    The ship, float and gliders carried sensors for *Chl F* and *b<sub>bp</sub>* that had been rigorously inter-  
3    calibrated, allowing us to directly compare optical measurements across all platforms. The float  
4    tracked a parcel of water, within the constraints discussed by Alkire et al. (2012). The gliders  
5    tracked the float, typically operating within 50 km of the float, although at the beginning of the  
6    experiment strong currents and eddies occasionally swept them further away. The timeline  
7    within the float patch showed a steady progression of increasing phytoplankton biomass  
8    beginning about YD 110 and continuing through the *Main Bloom* (Fig. 3A). The increase in  
9    biomass was accompanied by an increase in the optical community index, reflecting the  
10   beginning of the transition from wintertime pico- and nanophytoplankton to spring bloom  
11   diatoms (Fig. 3D); within the float patch, the optical index was relatively constant between YD  
12   118 – 132.

13   Initially, a similar pattern of low biomass was observed in data from all four gliders, but as the  
14   bloom progressed more than a five-fold variation was observed on any given day (Mahadevan et  
15   al., 2012). Not only was biomass patchy, but the optical community index was also patchy as the  
16   gliders (and ship during the May cruise) moved in and out of water parcels with different  
17   phytoplankton communities (Figs. 6A, 9A).

18   Through analysis of glider and model data, Mahadevan et al. (2012), showed that the springtime  
19   stratification is due to the action of submesoscale mixed layer eddies that drive a net horizontal  
20   transfer of lighter water above heavier water, thereby stratifying the mixed layer. This  
21   mechanism generates patches of shallower mixed layers as seen in Fig. 9B, resulting in patchy  
22   blooms. They speculated that different species might dominate in different patches, but they  
23   referenced patchiness only as biomass. Here we show patchiness in community composition,  
24   with the period of highest heterogeneity occurring after YD 115 and persisting for ~ 20 d (Fig.  
25   9C). Our observation is similar to that of d'Ovidio et al. (2010), who used satellite data to  
26   determine that submesoscale patches are short-lived (O(weeks)) ecological niches that allow  
27   different phytoplankton taxa to bloom.

28   Our observations raise the question as to the mechanism(s) of the observed patchiness in  
29   phytoplankton community composition. Is it a product of temporal offsets in bloom evolution in  
30   the various patches, related to restratification by submesoscale mixed layer eddies, or potential

1 nutrient injection (Levy et al., 2012)? Or to a lack of diatom bloom development in some water  
2 parcels, perhaps due to zooplankton patchiness or insufficient diatom seed populations? Or a  
3 combination of controlling factors? The float patch appeared to have persisted for the longest  
4 time period as a diatom community, although at least one glider briefly observed a diatom patch  
5 after the bloom terminated at the float (yellow dots on YD 147-148). The mechanism for diatom  
6 bloom termination might also differ among the different patches, controlled by patch-specific  
7 abiotic and biotic factors. One mechanisms of diatom bloom termination observed on board the  
8 ship was resting spore formation and sinking (Rynearson et al., 2013). This appeared to be  
9 widespread as judged by the dominance of these spores in sediment traps at depth. Regardless,  
10 from YD 140 to the end of the float mission 5 days later, all five autonomous platforms observed  
11 only the single phytoplankton community, i.e., Group 1.

12

## 13 **5 Conclusions**

14 Simple optical measurements made from autonomous platforms allow us to follow the variability  
15 in phytoplankton biomass ( $Chl F$ ) and POC concentration ( $b_{bp}$ ) on highly resolved spatial and  
16 temporal scales. The ratio of these optical measurements provides additional, more qualitative  
17 information about the plankton community composition. The interpretation of these ratios must  
18 be based on *in situ* validation and used within a limited set of conditions, at least until a better  
19 mechanistic understanding is developed. In late April the increase in the ratio  $Chl F/b_{bp}$  signaled  
20 a transition from a winter phytoplankton community dominated by pico- and nanophytoplankton  
21 to an early spring community dominated by diatoms. The observed shift in the optical index was  
22 primarily driven by the change in phytoplankton composition and distribution of biomass,  
23 reflecting differences in the taxa-specific chlorophyll-to-autotrophic carbon ratios.  
24 Furthermore, the optical index allowed us to observe changes in the physiological status of the  
25 community as well, clearly isolating the senescent, Si-limited, termination stage in the evolution  
26 of the phytoplankton-diatom bloom from surrounding patches of the same phytoplankton  
27 composition diatoms not yet in senescence. However, the changes in  $Chl F/b_{bp}$ , and by  
28 implication the transition in community composition, was not simultaneous over the spatial  
29 domain surveyed by the ship and gliders. The application of the optical index demonstrated that  
30 mesoscale and submesoscale variability in physical structures is reflected not only in total

1 biomass, but in community composition as well. Although our analysis did not manage to  
2 resolve the primary drivers of the observed spatial patchiness in community composition, the  
3 optical ratio approach offers a new tool set to study plankton patchiness *in-situ* on temporal and  
4 spatial scales relevant to ecosystem and biogeochemical research.

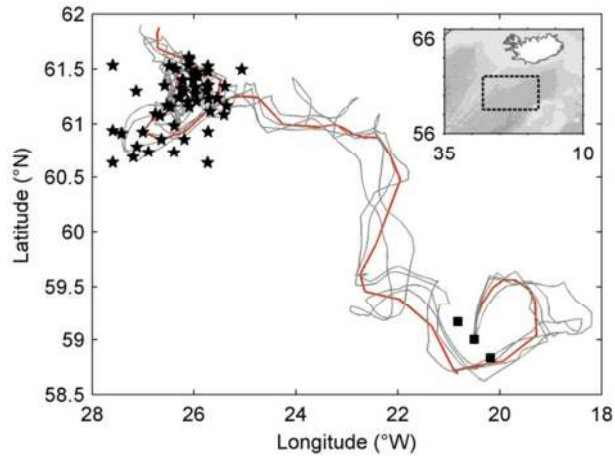
5

6

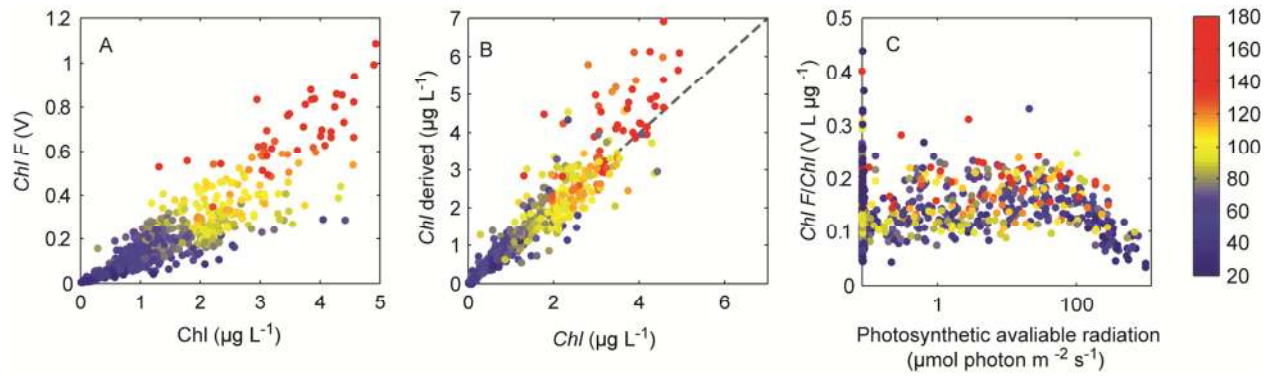
## 7 **Acknowledgements**

8 We thank Katherine Richardson for species data, Giorgio Dall’Olmo, Andrea Drzewianowski,  
9 Kristinn Gudmundsson, Emily Kallin, Eric Rehm, Michael Sauer, and Toby Westberry for help  
10 at sea and analyses, the University of Washington’s Applied Physics Lab Seaglider group, and  
11 the captain, crew and technicians of the *R/V Knorr* and *R/V S Bjarni Saemundsson*. This research  
12 was funded by the U.S. National Science Foundation (Grants OCE-0628107 and OCE-0628379)  
13 and NASA (Grants NNX-08AL92G and NNX-10AP29H).

14

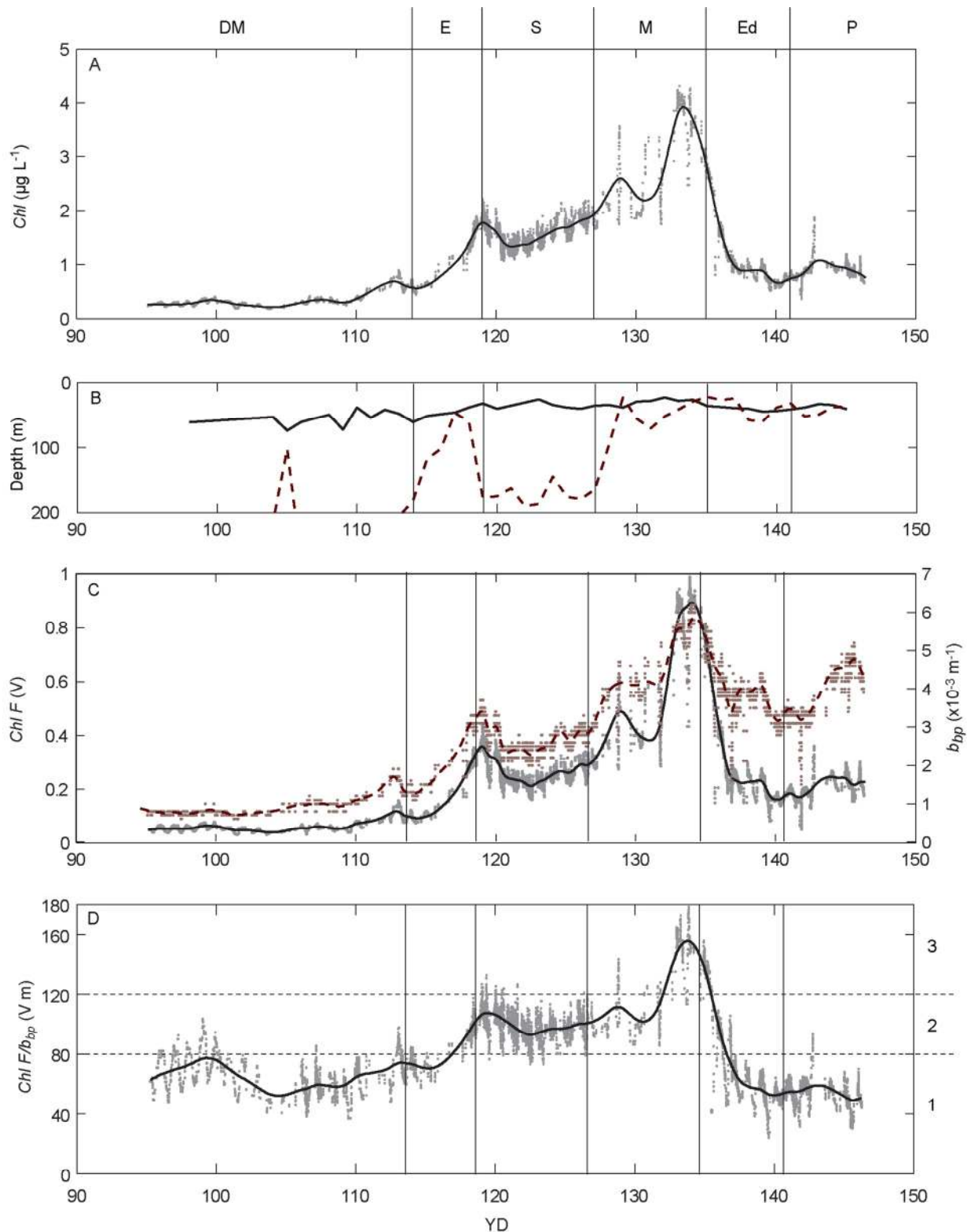


1  
 2 Figure 1. Map of NAB 2008 study area with the Lagrangian float path (red line) and four  
 3 Seaglider paths (gray lines). Autonomous platforms were deployed during the *R/S Bjarni*  
 4 *Saemundsson* cruise in early April 2008; squares indicate ship stations. Additional ship samples  
 5 were collected on a process cruise on the *R/V Knorr* in May 2008 (stars). Inset map indicates  
 6 study location relative to Iceland.  
 7



1  
 2 Figure 2. Chlorophyll data from *R/V Knorr* CTD profiles in May, color coded by the optical  
 3 community index,  $Chl F/b_{bp}$  (color bar on right; units are V m). (A)  $Chl F$  vs. extracted  
 4 chlorophyll concentration,  $Chl$ , was used to develop a non-linear best-fit function of temperature,  
 5 PAR, depth and YD for converting float  $Chl F$  to  $Chl$  (D'Asaro, 2011). (B) Best-fit derived  $Chl$   
 6 vs. extracted  $Chl$  shows deviation at higher concentrations (1:1 gray dashed line). (C)  $Chl F$   
 7 normalized to  $Chl$  exhibits photoquenching at high PAR (surface samples).

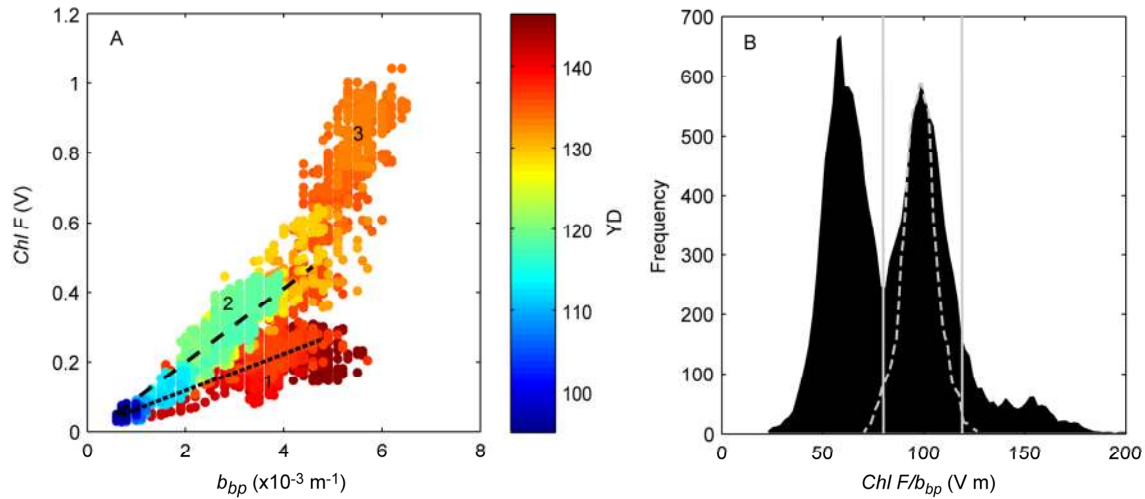
8



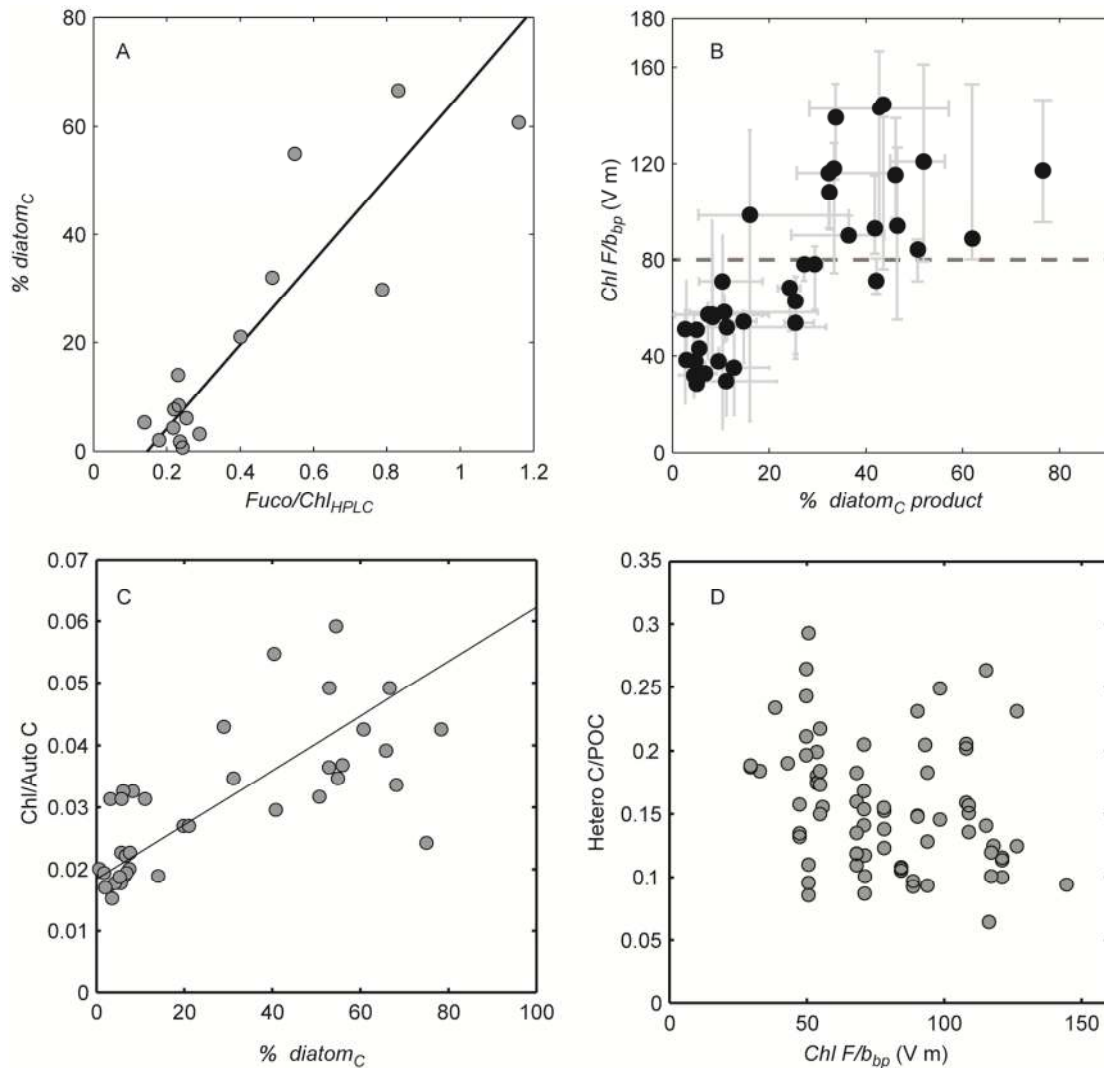
1  
 2 Figure 3. Float data collected for 10 – 50 m for YD 95 –146 (4 April to 25 May 2008). Vertical  
 3 lines and letters indicate periods in bloom evolution (see section 3.1); DM – Deep Mixing, E –  
 4 Early Bloom, S – Storm, M – Main Bloom, Ed – Eddy, P – Post Bloom defined in Section 3.1.

1 Dots represent initial median filtered data (7 point running median); superimposed line is  
2 smoothing spline fit (Matlab code *spaps.m*, smoothing parameter 0.1). (A) *Chl* derived from *Chl*  
3 *F*. (B) Mixed layer depth (dashed line) and depth of 0.415 mol photons m<sup>-2</sup> d<sup>-1</sup> isolume (solid  
4 line). (C) *Chl F* (~~line~~-solid line) and *b<sub>bp</sub>* (heavy solid line). (D) Optical community index, *Chl*  
5 *F/b<sub>bp</sub>*. Horizontal dashed lines indicate transitions between Groups 1 – 2 and 2 – 3. [Also see Fig.](#)  
6 [6](#).  
7



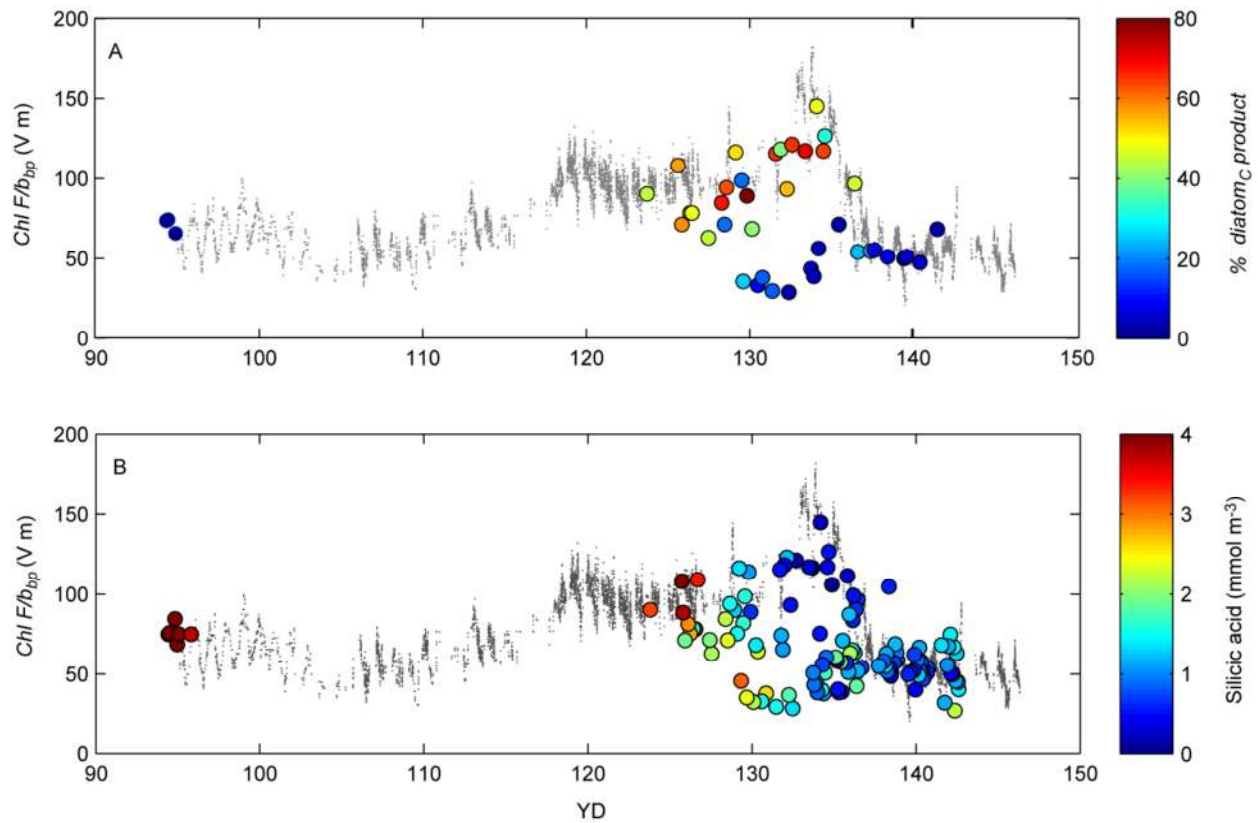


1  
 2 Figure 4. Optical community index and its components from entire float deployment; data from  
 3 10 – 50 m. (A)  $Chl F$  vs.  $b_{bp}$  shows three groups: Group 1 (dotted line); Group 2 (dashed line);  
 4 Group 3, no regression calculated. Some data points in Group 3 are obscured by Group 2. Color  
 5 coding is YD. (B) Frequency distribution of the optical community index (additional 2 point  
 6 median filter). Centroids corresponding to the regression lines in panel A. Gray dashed line  
 7 corresponds to the frequency distribution of the optical community index during period YD 120  
 8 – 127.  
 9



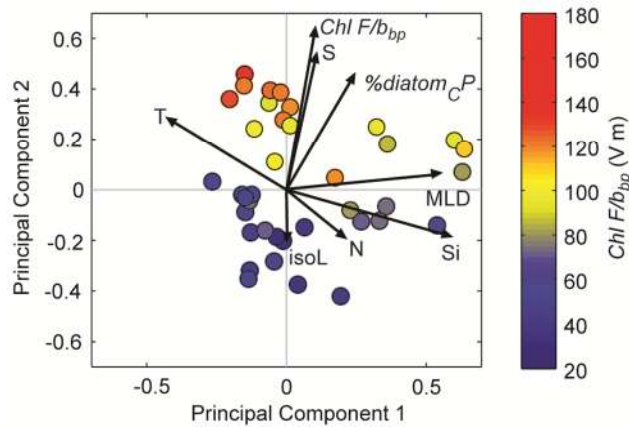
1  
 2 Figure 5. Community composition. Gray circles in Panels A, C and D are for individual water  
 3 samples; black circles in Panel B are averages for each profile. (A)  $\text{Fuco}/\text{Chl}_{\text{HPLC}}$  (g/g) is  
 4 correlated with  $\% \text{ diatom}_C$ . (B) Optical community index is related to phytoplankton community  
 5 composition, represented as  $\% \text{ diatom}_C \text{ product}$ . Bars are the range of individual values within  
 6 each profile; horizontal line indicates the division between Groups 1 and 2 based on Fig. 4B. (C)  
 7  $\text{Chl}$ -to-autotrophic carbon increases with the fraction of diatoms. (D) Ratio of heterotrophic  
 8 carbon biomass to total POC is not correlated with optical community index.

9



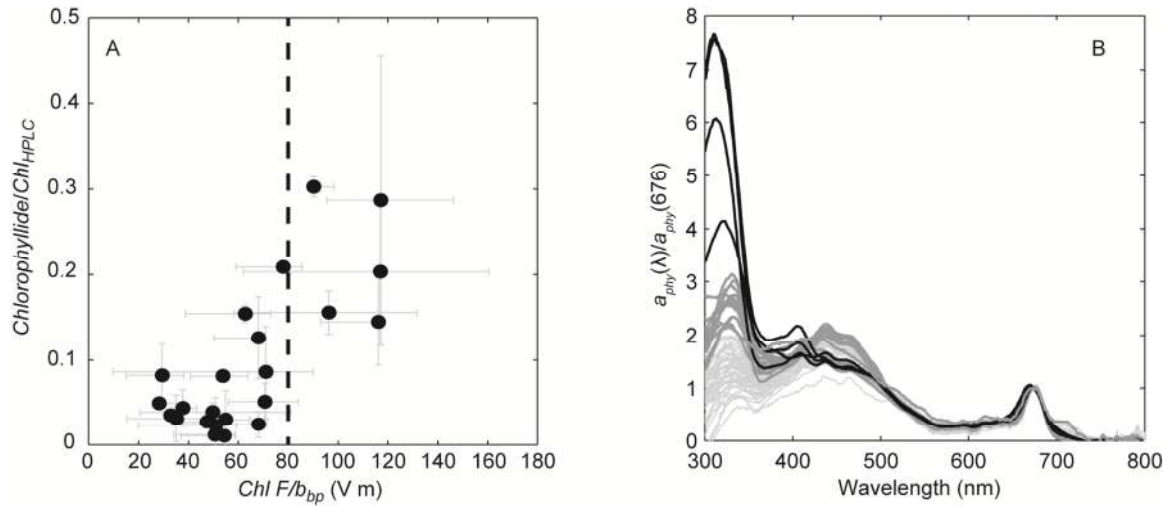
1  
 2 Figure 6. Optical community index,  $Chl F/b_{bp}$ , from ship CTD profiles (circles) superimposed on  
 3 float data (gray); 10 – 50 m median is plotted for each ship profile. (A) The optical community  
 4 index color coded by % *diatom<sub>C</sub> product* (n=42). The index was high when the relative diatom  
 5 abundance was high. (B) Same but color coded by Si concentration. Highest values of  $Chl F/b_{bp}$   
 6 were concurrent with lowest values of Si (n = 123).

7

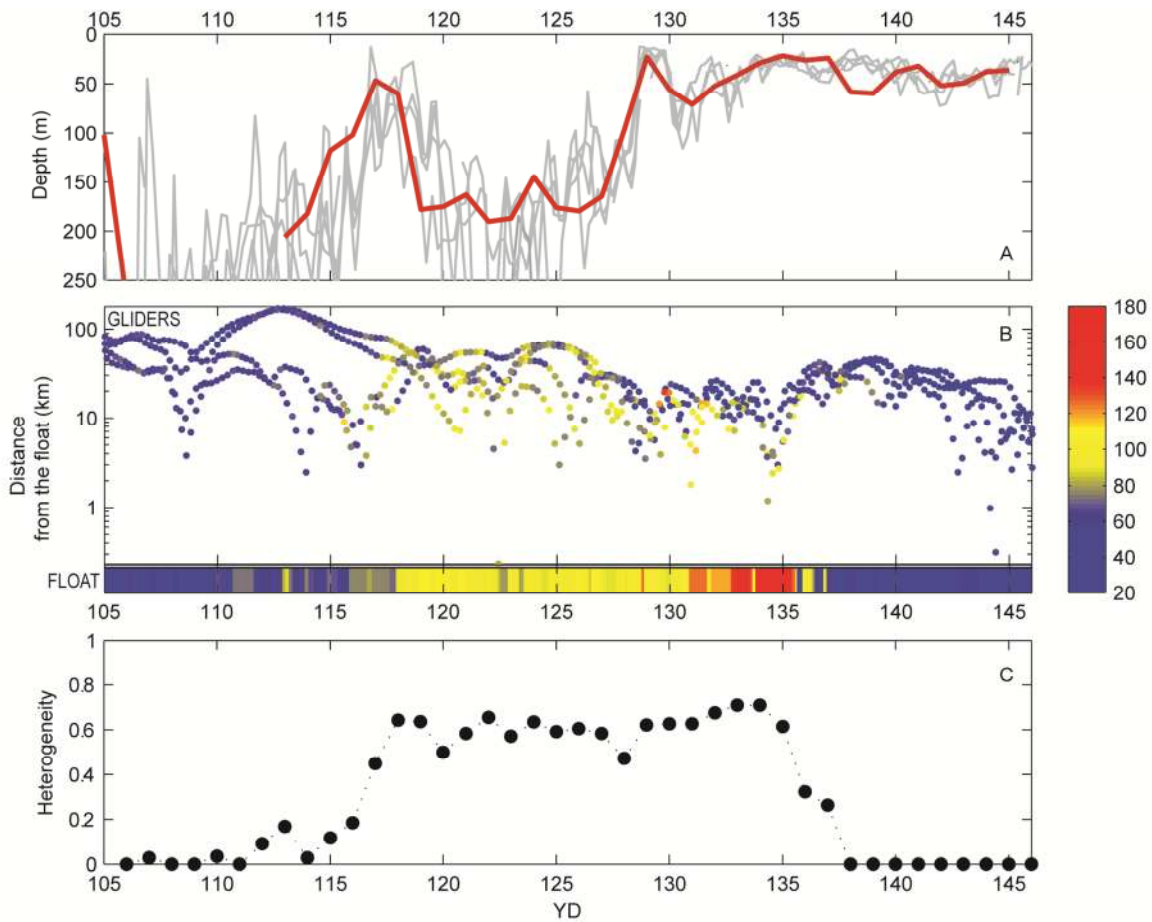


1  
 2 Figure 7. PCA biplot for *R/V Knorr* CTD stations ( $n = 38$ ), color coded by median  $Chl F/b_{bp}$  for  
 3 | 10-50 m, where blue corresponds to Group 1, yellow to Group 2 and red to Group 3. Together  
 4 | PCs 1 and 2 explain 68.7% of the variance. The length of a single parameter vector (black line  
 5 | with arrow) describes its loading contribution to the ~~on a~~ PC, while the direction of the vector,  
 6 | starting from the axes intersection, depicts the "biplot" gradient of the specific parameters: T –  
 7 | temperature, S – salinity, IsoL – 0.415 isolume depth, MLD – mixed layer depth, N – nitrate, Si  
 8 | – silicic acid,  $Chl F/b_{bp}$  – optical community index, and % *diatom*<sub>C</sub>*P* (here representing %  
 9 | *diatom*<sub>C</sub> product for brevity).

10



1  
 2 Figure 8. (A) Chlorophyllide concentration normalized to  $Chl_{HPLC}$  (g/g) was greater at higher  
 3 values of the optical community index. Bars are the range of individual samples within each  
 4 profile (23 profiles, 60 HPLC samples). (B) Phytoplankton absorption coefficient,  $a_{phy}$ ,  
 5 normalized to absorption at 676 nm; all available data are shown for completeness (n=63). Large  
 6 peaks near 300 nm occurred when the optical community index exceeded 80 V m (dark grey and  
 7 black lines); black lines note spectra with shifts in the absorption peak from 325 – 330 nm to 310  
 8 | – 315 nm.



1  
 2 Figure 9. Spatial heterogeneity in phytoplankton community composition, determined from four  
 3 gliders and the float. (A) Mixed layer depths, from gliders (gray line) and float (red line). (B)  
 4 Distances between gliders and Lagrangian float. Data are color coded as  $Chl F/b_{bp}$ ; dots  
 5 represent glider data and color bar at bottom represents float data. (C) Heterogeneity index for  
 6 community composition, defined in Section 2.4.

1 | Table 1. List of measured variables and methodologies, as measured on different platforms. .

<u>Parameter measured</u>	<u>Symbol /Acronym</u>	<u>Instrument or /method for specific platform</u>		
		<u>Ship</u>	<u>Lagrangian Float</u>	<u>Seagliders</u>
<u>Temperature, Conductivity (Salinity)</u>	<u>T, S</u>	<u>SBE 911plus</u>	<u>SBE 41</u>	<u>unpumped, custom -SBE CT sensor</u>
<u>Chlorophyll fluorescence</u>	<u>Chl F</u>	<u>WET Labs FLNTU</u>	<u>WET Labs FLNTU</u>	<u>WET Labs BB2F</u>
<u>Volume scattering function, calculated optical backscattering</u>	<u><math>\beta</math>(700 nm), <math>b_{bp}</math></u>	<u>WET Labs FLNTU</u>	<u>WET Labs FLNTU</u>	<u>WET Labs BB2F</u>
<u>Photosynthetically active radiation</u>	<u>PAR</u>	<u>Biospherical QSP2300</u>	<u>LI-COR 192-SA</u>	
<u>Nutrients: n; Nitrate and silicic acid</u>	<u>N, Si</u>	<u>Kallin et al. (2011), and Lachat (1996, 1999)</u>	<u>ISUS (not reported)</u>	
<u>Chlorophyll from ; fluorometric analysis extracts</u>	<u>Chl</u>	<u>Knap et al. (1996)</u>		
<u>Chlorophyll, HPLC analysis [MP1]</u>	<u>Chl<sub>HPLC</sub></u>	<u>Van Heukelem and Thomas (2001), Hooker et al. (2009)</u>		
<u>Phytoplankton absorption coefficient</u>	<u><math>a_{phy}(\lambda)</math></u>	<u>Mitchell and Kiefer (1988), Kishino et al., (1985)</u>		
<u>Phytoplankton cell carbon</u>		<u>Sieracki and Poulton (2011) and references therein</u>		
<u>Particulate organic carbon</u>	<u>POC</u>	<u>Cetinić et al. (2012)</u>		

2  
3

1 |

## 2 **References**

- 3 Alkire, M. B., D'Asaro, E., Lee, C., Perry, M. J., Gray, A., Cetinic, I., Briggs, N., Rehm, E.,  
4 Kallin, E., Kaiser, J., and Gonzalez-Posada, A.: Estimates of net community production and  
5 export using high-resolution, Lagrangian measurements of O<sub>2</sub>, NO<sub>3</sub><sup>-</sup>, and POC through the  
6 evolution of a spring diatom bloom in the North Atlantic, Deep-Sea Research Part I-  
7 Oceanographic Research Papers, 64, 157-174, 10.1016/j.dsr.2012.01.012, 2012.
- 8 Behrenfeld, M. J., Boss, E., Siegel, D. A., and Shea, D. M.: Carbon-based ocean productivity and  
9 phytoplankton physiology from space, Global Biogeochemical Cycles, 19, -, 2005.
- 10 Boss, E., and Behrenfeld, M.: In situ evaluation of the initiation of the North Atlantic  
11 phytoplankton bloom, Geophysical Research Letters, 37, L18603, 10.1029/2010gl044174, 2010.
- 12 Bricaud, A., Babin, M., Morel, A., and Claustre, H.: Variability in the Chlorophyll-Specific  
13 Absorption-Coefficients of Natural Phytoplankton - Analysis and Parameterization, Journal of  
14 Geophysical Research-Oceans, 100, 13321-13332, 1995.
- 15 Briggs, N.: Backscatter\_Calibration-NAB08,  
16 <http://osprey.bcodmo.org/dataset.cfm?id=13820&flag=view> Biol. and Chem. Oceanogr. Data  
17 Manage. Office, Woods Hole, Mass., 2011.
- 18 Briggs, N., Perry, M. J., Cetinic, I., Lee, C., D'Asaro, E., Gray, A., and Rehm, E.: High-  
19 resolution observations of aggregate flux during a sub-polar North Atlantic spring bloom, Deep  
20 Sea Research Part I: Oceanographic Research Papers, 58, 1031-1039, 10.1016/j.dsr.2011.07.007,  
21 2011.
- 22 Bucciarelli, E., and Sunda, W. G.: Influence of CO<sub>2</sub>, nitrate, phosphate, and silicate limitation on  
23 intracellular dimethylsulfoniopropionate in batch cultures of the coastal diatom *Thalassiosira*  
24 *pseudonana*, Limnology and Oceanography, 48, 2256-2265, 2003.
- 25 Burger, W., and Burge, M. J.: Digital image processing: an algorithmic introduction using Java,  
26 Springer, New York, 2008.
- 27 Campbell, L., Henrichs, D.W., Olson, R.J., and Sosik, H.M.: Continuous automated imaging-in-  
28 flow cytometry for detection and early warning of *Karenia brevis* blooms in the Gulf of Mexico,  
29 Environmental Science and Pollution Research, 20, 6896 – 6902, 10.1007/s11356-012-1437-4,  
30 2013.
- 31 Cetinić, I., Perry, M. J., Briggs, N. T., Kallin, E., D'Asaro, E. A., and Lee, C. M.: Particulate  
32 organic carbon and inherent optical properties during 2008 North Atlantic Bloom Experiment, J.  
33 Geophys. Res., 117, C06028, 10.1029/2011jc007771, 2012.
- 34 Chang, F., Chen, C. J., and Lu, C. J.: A linear-time component-labeling algorithm using contour  
35 tracing technique, Computer Vision and Image Understanding, 93, 206-220, 2004.
- 36 Cleveland, J., and Perry, M.: Quantum yield, relative specific absorption and fluorescence in  
37 nitrogen-limited *Chaetoceros gracilis*, Marine Biology, 94, 489-497, 1987.
- 38 D'Asaro, E.: Chlorophyll\_Calibration-NAB08,  
39 <http://osprey.bcodmo.org/dataset.cfm?id=13820&flag=view> Biol. and Chem. Oceanogr. Data  
40 Manage. Office, Woods Hole, Mass., 2011.



1 D'Asaro, E. A.: Performance of autonomous Lagrangian floats, *Journal of Atmospheric and*  
2 *Oceanic Technology*, 20, 896-911, 2003.

3 d'Ovidio, F., De Monte, S., Alvain, S., Dandonneau, Y., and Lévy, M.: Fluid dynamical niches  
4 of phytoplankton types, *Proceedings of the National Academy of Sciences*, 107, 18366-18370,  
5 10.1073/pnas.1004620107, 2010.

6 Denman, K. L., and Platt, T.: The variance spectrum of phytoplankton in a turbulent ocean, *J.*  
7 *mar. Res.*, 34, 593-601, 1976.

8 Ducklow, H. W., and Harris, R. P.: Introduction to the JGOFS North Atlantic bloom experiment  
9 *Deep-Sea Research Part II Topical Studies in Oceanography*, 40, 1-8, 1993.

10 Egge, J. K., and Aksnes, D. L.: Silicate as Regulating Nutrient in Phytoplankton Competition,  
11 *Mar Ecol-Prog Ser*, 83, 281-289, 1992.

12 Eriksen, C. C., Osse, T. J., Light, R. D., Wen, T., Lehman, T. W., Sabin, P. L., Ballard, J. W.,  
13 and Chiodi, A. M.: Seaglider: a long-range autonomous underwater vehicle for oceanographic  
14 research, *Oceanic Engineering, IEEE Journal of*, 26, 424-436, 2001.

15 Fujiki, T., and Taguchi, S.: Variability in chlorophyll a specific absorption coefficient in marine  
16 phytoplankton as a function of cell size and irradiance, *J. Plankton Res.*, 24, 859-874,  
17 10.1093/plankt/24.9.859, 2002.

18 Geider, R. J.: Light and temperature-dependence of the carbon to chlorophyll-a ratio in  
19 microalgae and cyanobacteria - implications for physiology and growth of phytoplankton, *New*  
20 *Phytol.*, 106, 1-34, 10.1111/j.1469-8137.1987.tb04788.x, 1987.

21 Gordon, L. I., Joe C. Jennings, J., Ross, A. A., and Krest, J. M.: A suggested protocol for  
22 continuous flow automated analysis of seawater nutrients (Phosphate, Nitrate, Nitrite and Silicic  
23 Acid) in the WOCE Hydrographic Program and the Joint Global Ocean Fluxes Study. 92-1,  
24 1992.

25 Head, E. J. H., and Horne, E. P. W.: Pigment Transformation and Vertical Flux in an Area of  
26 Convergence in the North-Atlantic, *Deep-Sea Research Part II-Topical Studies in Oceanography*,  
27 40, 329-346, 1993.

28 Hooker, S. B., Heukelem, L. V., Thomas, C. S., Claustre, H., Ras, J., Schlüter, L., Clementson,  
29 L., van der Linde, D., Eker-Develi, E., Berthon, J.-F., Barlow, R., Sessions, H., Ismail, H., and  
30 Perl, J.: The Third SeaWiFS HPLC Analysis Round-Robin Experiment (SeaHARRE-3),  
31 National Aeronautics and Space Administration, Goddard, 2009.

32 IOC: First IODE Workshop on Quality Control of Chemical Oceanographic Data Collections,  
33 UNESCO, Paris, 2010.

34 Jeffrey, S. W.: Algal pigment systems, in: *Primary productivity in the sea*, edited by: Falkowski,  
35 P. G., Plenum Publishing Corporation, New York, 33-57, 1980.

36 Jeffrey, S. W., and Hallegraeff, G. M.: Chlorophyllase Distribution in 10 Classes of  
37 Phytoplankton - a Problem for Chlorophyll Analysis, *Mar Ecol-Prog Ser*, 35, 293-304, 1987.

38 Kallin, E., Cetinic, I., Perry, M. J., and Sauer, M.: Laboratory\_analysis\_report-NAB08,  
39 <http://osprey.bcodmo.org/project.cfm?flag=view&id=102&sortby=project> Biol. and Chem.  
40 *Oceanogr. Data Manage. Office*, Woods Hole, Mass. , 2011.

- 1 Kishino, M., Takahashi, M., Okami, N., and Ichimura, S.: Estimation of the spectral absorption  
2 coefficients of phytoplankton in the sea, *Bulletin of Marine Science*, 37, 634-642, 1985.
- 3
- 4
- 5 [Knap, A., Michaels, A., Close, A., Ducklow, H. and Dickson, A. \(eds\): Protocols for the Joint  
6 Global Ocean Flux Study \(JGOFS\) Core Measurements. JGOFS Report N. 19, vi + 170 pp.  
7 Reprint of the 10C Manuals and Guides No 29, UNESCO 1994, 1996.](#)
- 8 Kruskopf, M., and Flynn, K. J.: Chlorophyll content and fluorescence responses cannot be used  
9 to gauge reliably phytoplankton biomass, nutrient status or growth rate, *New Phytol.*, 169, 525-  
10 536, 10.1111/j.1469-8137.2005.01601.x, 2006.
- 11 Lachat, I.: Silicate in brackish or seawater -- QuickChem Method 31-114-27-1-B, Lachat  
12 Instruments, Milwaukee, WI, 1996.
- 13 Lachat, I.: Nitrate and/or nitrite in brackish or seawater -- QuickChem Method 31-107-04-1-A,  
14 Lachat Instruments, Milwaukee, WI, 1999.
- 15 Letelier, R. M., Karl, D. M., Abbott, M. R., and Bidigare, R. R.: Light driven seasonal patterns of  
16 chlorophyll and nitrate in the lower euphotic zone of the North Pacific Subtropical Gyre,  
17 *Limnology and Oceanography*, 49, 508-519, 2004.
- 18 Levy, M., R. Ferrari, P. J.S. Franks, A. P. Martin, and Rivière, P.: Bringing physics to life at the  
19 submesoscale, *Geophysical Research Letters*, 10.1029/2012GL052756, 2012.
- 20 Li, Q. P., Franks, P. J., Landry, M. R., Goericke, R., and Taylor, A. G.: Modeling phytoplankton  
21 growth rates and chlorophyll to carbon ratios in California coastal and pelagic ecosystems,  
22 *Journal of Geophysical Research: Biogeosciences* (2005–2012), 115, 2010.
- 23 Lippemeier, S., Hartig, P., and Colijn, F.: Direct impact of silicate on the photosynthetic  
24 performance of the diatom *Thalassiosira weissflogii* assessed by on- and off-line PAM  
25 fluorescence measurements, *Journal of Plankton Research*, 21, 269-283, 1999.
- 26 Llewellyn, C. A., Fishwick, J. R., and Blackford, J. C.: Phytoplankton community assemblage in  
27 the English Channel: a comparison using chlorophyll a derived from HPLC-CHEMTAX and  
28 carbon derived from microscopy cell counts, *Journal of Plankton Research*, 27, 103-119,  
29 10.1093/plankt/fbh158, 2005.
- 30 Llewellyn, C. A., Tarran, G. A., Galliène, C. P., Cummings, D. G., De Menezes, A., Rees, A. P.,  
31 Dixon, J. L., Widdicombe, C. E., Fileman, E. S., and Wilson, W. H.: Microbial dynamics during  
32 the decline of a spring diatom bloom in the Northeast Atlantic, *Journal of Plankton Research*, 30,  
33 261-273, 10.1093/plankt/fbm104, 2008.
- 34 Llewellyn, C. A., and Airs, R. L.: Distribution and abundance of MAAs in 33 species of  
35 microalgae across 13 classes, *Marine Drugs*, 8, 1273-1291, 2010.
- 36 Loisel, H., Vantrepotte, V., Norkvist, K., Meriaux, X., Kheireddine, M., Ras, J., Pujo-Pay, M.,  
37 Combet, Y., Leblanc, K., Dall'Olmo, G., Mauriac, R., Dessailly, D., and Moutin, T.:  
38 Characterization of the bio-optical anomaly and diurnal variability of particulate matter, as seen  
39 from scattering and backscattering coefficients, in ultra-oligotrophic eddies of the Mediterranean  
40 Sea, *Biogeosciences*, 8, 3295-3317, 10.5194/bg-8-3295-2011, 2011.

- 1 Lorenzen, C. J.: A method for the continuous measurement of the in vivo chlorophyll  
2 concentration, *Deep-Sea Res*, 13, 223-227, 1966.
- 3 Lorenzen, C. J.: Determination of chlorophyll and phaeo-pigments: spectrophotometric equations,  
4 *Limnology and Oceanography*, 12, 343-346, 1967.
- 5 Mahadevan, A., D'Asaro, E., Lee, C., and Perry, M. J.: Eddy-Driven Stratification Initiates  
6 North Atlantic Spring Phytoplankton Blooms, *Science*, 337, 54-58, 10.1126/science.1218740,  
7 2012.
- 8 Marra, J.: Analysis of diel variability in chlorophyll fluorescence, *Journal of Marine Research*,  
9 55, 767-784, 10.1357/0022240973224274, 1997.
- 10 Martin-Jezequel, V., Hildebrand, M., and Brzezinski, M. A.: Silicon metabolism in diatoms:  
11 Implications for growth, *Journal Of Phycology*, 36, 821-840, 10.1046/j.1529-8817.2000.00019.x,  
12 2000.
- 13 Matrai, P. A., Steele, M., Swift, D., Riser, S., Johnson, K. S., and Breckenridge, L.:  
14 Autonomous observations of arctic phytoplankton activity: The first annual cycle in ice-covered  
15 waters, *International Ocean Colour Science Meeting 2013*, Darmstadt, Germany, 2013.
- 16 Menden-Deuer, S., and Lessard, E. J.: Carbon to volume relationships for dinoflagellates,  
17 diatoms, and other protist plankton, *Limnology and Oceanography*, 45, 569-579, 2000.
- 18 Mitchell, B. G., and Kiefer, D. A.: Chlorophyll a specific absorption and fluorescence excitation  
19 spectra for light-limited phytoplankton, *Deep-Sea Research, Part 1*, 35, 639-663, 1988.
- 20 Moisan, T. A., Sathyendranath, S., and Bouman, H. A.: Ocean color remote sensing of  
21 phytoplankton functional types, *Remote sensing of biomass—principles and applications*. Intech,  
22 Rijeka, Croatia, 101-122, 2012.
- 23 Moore, C. M., Lucas, M. I., Sanders, R., and Davidson, R.: Basin-scale variability of  
24 phytoplankton bio-optical characteristics in relation to bloom state and community structure in  
25 the Northeast Atlantic, *Deep Sea Research Part I: Oceanographic Research Papers*, 52, 401-419,  
26 2005.
- 27 Munk, W.: *Oceanography before, and after, the advent of satellites*, Elsevier Oceanography  
28 Series, 63, 1-4, 2000.
- 29 Nencioli, F., Chang, G., Twardowski, M., and Dickey, T. D.: Optical Characterization of an  
30 Eddy-induced Diatom Bloom West of the Island of Hawaii, *Biogeosciences*, 7, 151-162, 2010.
- 31 O'Reilly, J. E., Maritorena, S., Mitchell, B. G., Siegel, D. A., Carder, K. L., Garver, S. A., Kahru,  
32 M., and McClain, C.: Ocean color chlorophyll algorithms for SeaWiFS, *Journal of Geophysical  
33 Research-Oceans*, 103, 24937-24953, 1998.
- 34 Olson, R. J., and Sosik, H. M.: A submersible imaging-in-flow instrument to analyze nano-and  
35 microplankton: Imaging FlowCytobot, *Limnol. Oceanogr. Methods*, 5, 195-203, 2007.
- 36 Perry, M. J., Sackmann, B. S., Eriksen, C. C., and Lee, C. M.: Seaglider observations of blooms  
37 and subsurface chlorophyll maxima off the Washington coast, *Limnology and Oceanography*,  
38 53, 2169-2179, 2008.
- 39 Putland, J., and Iverson, R.: Phytoplankton biomass in a subtropical estuary: distribution, size  
40 composition, and carbon: chlorophyll ratios, *Estuaries and coasts*, 30, 878-885, 2007.

- 1 Ridout, P., and Morris, R.: Short-term variations in the pigment composition of a spring  
2 phytoplankton bloom from an enclosed experimental ecosystem, *Marine Biology*, 87, 7-11,  
3 1985.
- 4 Roesler, C. S., and Barnard, A. H.: Optical proxy for phytoplankton biomass in the absence of  
5 photophysiology: Rethinking the absorption line height, *Methods in Oceanography*, 2014.
- 6 Rose, J. M., Caron, D. A., Sieracki, M. E., and Poulton, N.: Counting heterotrophic  
7 nanoplanktonic protists in cultures and aquatic communities by flow cytometry, *Aquatic*  
8 *Microbial Ecology*, 34, 263-277, 2004.
- 9 Ryan, J., Greenfield, D., Marin III, R., Preston, C., Roman, B., Jensen, S., Pargett, D., Birch, J.,  
10 Mikulski, C., and Doucette, G.: Harmful phytoplankton ecology studies using an autonomous  
11 molecular analytical and ocean observing network, *Limnology and Oceanography*, 56, 1255-  
12 1272, 2011.
- 13 Rynearson, T. A., K. Richardson, R. S. Lampitt, M. E. Sieracki, A. J. Poulton, M. M.  
14 Lyngsgaard, and M. J. Perry. Major contribution of diatom resting spores to sinking flux in the  
15 sub-polar North Atlantic. *Deep-Sea Research, Part I Oceanographic Research Papers*. 82:60-71,  
16 2013.
- 17 Sackmann, B. S., Perry, M. J., and Eriksen, C. C.: Seaglider observations of variability in  
18 daytime fluorescence quenching of chlorophyll-a in Northeastern Pacific coastal waters,  
19 *Biogeosciences Discuss.*, 5, 2839-2865, 10.5194/bgd-5-2839-2008, 2008.
- 20 Sieracki, M. E., Viles, C. L., and Webb, K. L.: Algorithm to Estimate Cell Biovolume Using  
21 Image Analyzed Microscopy, *Cytometry*, 10, 551-557, 1989.
- 22 Sieracki, M. E., and Poulton, N.: *Phytoplankton\_Carbon-NAB08*,  
23 <http://osprey.bcodmo.org/project.cfm?flag=view&id=102&sortby=project> Biol. and Chem.  
24 Oceanogr. Data Manage. Office, Woods Hole, Mass. , 2011.
- 25 Sigleo, A., Neale, P. J., and Spector, A.: Phytoplankton pigments at the Weddell–Scotia  
26 confluence during the 1993 austral spring, *Journal of Plankton Research*, 22, 1989-2006, 2000.
- 27 Sosik, H. M., and Olson, R. J.: Automated taxonomic classification of phytoplankton sampled  
28 with imaging-in-flow cytometry, *Limnol. Oceanogr. Methods*, 5, 204-216, 2007.
- 29 Strutton, P. G., Martz, T. R., DeGrandpre, M. D., McGillis, W. R., Drennan, W. M., and Boss,  
30 E.: Bio-optical observations of the 2004 Labrador Sea phytoplankton bloom, *J. Geophys. Res.*,  
31 116, C11037, 10.1029/2010jc006872, 2011.
- 32 Sullivan, J. M., Twardowski, M., Zaneveld, J. R., and Moore, C.: Measuring optical  
33 backscattering in water. *In* A. A. Kokhanovsky (Ed.), *Light Scattering Reviews* 7 (pp. 189–224).  
34 Springer Berlin Heidelberg, 2013.
- 35 Twardowski, M. S., Claustre, H., Freeman, S. A., Stramski, D., and Huot, Y.: Optical  
36 backscattering properties of the 'clearest' natural waters, *Biogeosciences*, 4, 1041-1058, 2007.
- 37 Van Heukelem, L., and Thomas, C. S.: Computer-assisted high-performance liquid  
38 chromatography method development with applications to the isolation and analysis of  
39 phytoplankton pigments, *Journal of Chromatography A*, 910, 31-49, 2001.

- 1 Veldhuis, M. J. W., Cucci, T. L., and Sieracki, M. E.: Cellular DNA content of marine  
2 phytoplankton using two new fluorochromes: Taxonomic and ecological implications, *Journal*  
3 *Of Phycology*, 33, 527-541, 1997.
- 4 Verity, P. G., Robertson, C. Y., Tronzo, C. R., Andrews, M. G., Nelson, J. R., and Sieracki, M.  
5 E.: Relationship between cell-volume and the carbon and nitrogen content of marine  
6 photosynthetic nanoplankton, *Limnology and Oceanography*, 37, 1434-1446, 1992.
- 7 Verity, P.G., Stoecker, D.K., Sieracki, M.E., Burkill, P.H., Edwards, E.S., and Tronzo, C.R.:  
8 Abundance, Biomass and Distribution of Heterotrophic Dinoflagellates During the North-  
9 Atlantic Spring Bloom, *Deep-Sea Research Part II Topical Studies in Oceanography*, 40, 227-  
10 244, 1993.
- 11 Yoder, J. A., McClain, C. R., Blanton, J. O., and Oey, L. Y.: Spatial scales in CZCS-chlorophyll  
12 imagery of the southeastern US continental shelf, *Limnology and Oceanography*, 929-941, 1987.
- 13 Zhang, X., Hu, L., and He, M.-X.: Scattering by pure seawater: Effect of salinity, *Opt. Express*,  
14 17, 5698-5710, 2009.